STUDIES OF COMPOUND STATES OF NEGATIVE IONS USING LASER BEAMS*

R. N. Compton and C. S. Feigerle
Department of Chemistry, The University of Tennessee
Knoxville, Tennessee 37996

and
Chemical Physics Section, Oak Ridge National Laboratory,
Oak Ridge, Tennessee 37831-6125

and
H. P. Saha
Department of Physics, University of Central Florida
Orlando, Florida 32816-0993

* **This Document is for Unrestricted Dissemination**

This represents the final report of the research performed for the Office of Naval Research under Grant No. ONR N-00014-89-J-1787. Although this report is to cover only the period from 4/1/89 to 12/31/91, we will include selected items from the previous grant No. ONR N-0014-87-K-0065 in order to provide continuity between the two. By all measures of performance, this research project has been an enormous success. Over ten major publications have resulted from this program. Seven of these publications have appeared in Physical Review Letters. This project has supported two post doctoral students and three graduate students. In addition, it has contributed to the scientific and professional advancement of associate professors, C. S. Feigerle of the University of Tennessee and H. P. Saha of the University of Central Florida. Two student have completed their Ph.D. dissertation in this program and another is scheduled to receive his in the summer of 1992.

This program has helped to launch the scientific careers of two former post doctoral students. Dr. Thomas J. Kavale, a post doctoral student from the University of Missouri, was

responsible for the studies of Be^- and He_2^-. He is continuing these studies at the University of Toledo where he has been very successful in the atomic physics community. Tom has been able to support his program through DOE. A second post doctoral student from Rice University, Dr. Howard S. Carman, Jr. was involved in studies of high power laser multiphoton ionization spectroscopy. His studies of photoelectron angular distribution (PADs) for cesium was the first clear demonstration of relativistic effects on PADs. Howard is now a permanent employee of the Oak Ridge National Laboratory. Dr. Adila Dodhy, a former graduate student from Auburn University, was also involved in high power laser multiphoton ionization studies. She is now employed at the Max Planck Institute in Germany. Dr. Perry Blazewicz, a graduate student from Yale University, completed his Ph.D. dissertation on multiphoton ionization of rare gases under the ONR support. He is presently a chemistry professor at the University of Puget Sound and Pacific Lutheran College.

The research performed on this grant is adequately described in the appended reprints. The significance of this program is underlined by the large number of Physical Review Letter articles, publications which are reserved for those studies of significant and wide spread scientific interest. We will summarize most of these below pointing out only the most significant results. The front page only of pertinent publications prior to 1990 are included as an appendix.

Experimental and Theoretical Studies of He^- $^4P^e$ and He_2^- ($^4\Pi_g$)

Much of our experimental effort has been devoted to understanding the structure and dynamics of the He^- $^4P^e$ ion. Previously we had observed its energy level [R. N. Compton, G. D. Alton, and D. J. Pegg, J. Phys. B 13, L651 (1980)] and measured its auto-detachment lifetime.

More recently, we have measured partial cross sections [D. J. Pegg, J. S. Thompson, J. Dellwo, R. N. Compton, and G. D. Alton, Phys. Rev. Lett. 64, 278 (1990)] and angular distributions [J. S. Thompson, D. J. Pegg, R. N. Compton, and G. D. Alton, J. Phy. B 23, L15 (1990)] for the photodetachment of electrons from the metastable He^- $^4P^e$ negative ion.

Our studies of He^- $^4P^e$ were culminated with a recent theoretical study of the photophysics of He^- $^4P^e$ [H. P. Saha and R. N. Compton, Phy. Rev. Lett. 64, 1510 (1990)]. In this study the multiconfiguration Hartree-Fock method which includes the effects of dynamical core polarization and electron correlation was used to calculate the photo-detachment cross

sections and asymmetry parameter ($\beta_{n,\ell}$) for both the 2s and 2p electrons. Excellent agreement was found with previously measured values in the limited range of the experiment. This was a *tour de force* calculation and in the words of one referee, "will become a classic."

Shortly after learning that He_2^- ions had been observed at Stanford Research Institute, we immediately began studies of the properties of this new and unexpected ion. We were able to employ fast-beam autodetachment spectroscopy studies of (30 - 65 KeV) He_2^- ion beams in order to measure the electron affinity of He_2 ($a^3\Sigma_u^+$). We found that He_2^- ($^4\Pi$) in the v = 1 state autodetached to He_2 $(a^3\Sigma_u^+)_{v=0}$ + e. In the center of mass frame this electron energy is exceedingly small, however, using the kinematic shift of the fast He_2^- ion beam allowed us to accurately measure those electrons which autodetach in the forward and backward direction of the center of mass system. In order to complete these experiments, it was necessary to measure the autodetachment energy for the isotope $^3He_2^-$ $(^4\Pi)_{v=1}$ as well as $^4He_2^-$ $(^4\Pi)_{v=1}$. Fortunately, the ORNL Physics Division had a tank of ^3He left over from the war years. We calculated that in order to replace our sample with a commercial source would have cost $\sim 10^6$ dollars. From these studies we obtained an electron affinity of 0.175 $\pm$ 0.032eV for the $^4He_2$ ($a^3\Sigma_u^+$) state by comparison of the $^3He_2^-$ and $^4He_2^-$ spectra. In addition to vibrational autodetachment we also observed the novel autodetachment of He_2^- into the He_2 ($x^1\Sigma_g^+$) + e repulsive continuum. This last observation has been the subject of numerous recent theoretical calculations.

As a result of the above studies we have contributed heavily to the understanding of the properties of He^- ($^4P^\circ$) and He_2^- ($^4\Pi$). These ions are of theoretical as well as practical interest. He^- ($^4P^\circ$) is used in tandem accelerators throughout the world.

Experimental Studies of Be^- ^4P and Ca^- $(4s^24p)^2P^\circ$

Previously in our ONR grant we reported the first experimental measurement of the energy level for the metastable Be^- $(1s^22s2p^2)^4P$ state at 2.53 $\pm$ 0.09eV. Fast beam autodetachment spectroscopy was employed in which collisional detachment was used to accurately determine the electron energy scale calibration [T. J. Kavale, G. D. Alton, R. N. Compton, D. J. Pegg, and J. S. Thompson, Phy. Rev. Lett. 55, 484 (1985)].

In 1987, we reported the first experimental evidence for a stable negative ion of calcium [D. J. Pegg, J. S. Thompson, R. N. Compton, and G. D. Alton, Phys. Rev. Lett. 59, 2267 (1987)]. This was the first report of a stable negative ion for a group II A element. In addition

we employed negative ion photoelectron spectroscopy to determine the electron affinity of Ca to be 0.043 ± 0.007eV. Many theoretical calculations have ensued which agree with this electron affinity. A recent experimental value (J. R. Peterson, to be published) places the EA somewhat lower. Both experiments agree that the EA is positive. This research was cited in numerous popular press and newspaper articles.

Laser Multiphoton Ionization of Atoms

In addition to studies of laser photodetachment of negative ions, this research has been concerned with high power laser multiphoton ionization photoelectron spectroscopy of atoms. Below we will briefly describe the more important results of this research.

In the first study, Ms. Adila Dodhy's Ph.D. thesis (Auburn University) was devoted to multiphoton ionization photoelectron angular distributions for alkali atoms. In particular, photoelectron angular distributions were measured for non-resonant two-photon ionization of cesium and rubidium atoms just above the ionization threshold [A. Dodhy, R. N. Compton, and J. A. D. Stockdale, Phy. Rev. Lett. 54, 422 (1985)]. The results compared favorably with theoretical estimates based upon non-relativistic atomic wave functions. Other papers in this general area were published.

The Ph.D. thesis of Dr. P. Blazewicz (Yale University) reported the first photoelectron angular distributions from resonantly enhanced multiphoton ionization of xenon via the $6s[3/2]^0_1$ and $6s'[1/2]^0_1$ states [P. R. Blazewicz, X. Tang, R. N. Compton, and J. A. D. Stockdale, J. Opt. Soc. Am. B4, 770 (1987)]. Again theory was included in the analysis.

The Ph.D. thesis of Mr. L. E. Cuéllar (University of Tennessee) will include MPI studies of alkali atoms. One of his studies involved the first measurements of photoelectron angular distribution for ns (n = 8-12) subshells of cesium [L. E. Cuéllar, R. N. Compton, H. S. Carman, Jr., and C. S. Feigerle, Phy. Rev. Lett. 65, 163 (1990)]. In a separate study Mr. Cuéllar reported the first circular dichroism effect in photoelectron angular distributions for an atom [L. E. Cuéllar, C, S. Feigerle, H. S. Carman, Jr., and R. N. Compton, Phy. Rev. A 43, 6437 (1991)]. Both of these studies represent the very first measurements in the field. Other publications are being prepared. Mr. Cuéllar expects to graduate this summer.

The benefactors of the ONR grant are very appreciative of the unconditional support of Dr. Bobby Junker and Dr. Peter Reynolds of the Office of Naval Research. We feel that the

success of our research is partly due to the flexibilty, interest and support these contract monitors have demonstrated over the past few years. In addition to the research published, which is included as publications, we list other measures of success below.

Ph. D. Thesis

Adila Dodhy, "Photoelectron Angular Distributions for Cesium, Rubidium, and Sodium Atoms using Multiphoton Ionization" Auburn University, 1987.

Perry Blazewicz, "Multiphoton Ionization and Third-Harmonic Generation in Krypton and Xeron" Yale University, 1988.

Luis Cuéllar, "Multiphoton Ionization of Alkali Atoms" The University of Tennessee, in progress.

Awards

R. N. Compton, J. W. Beams Award (1991) for studies of negative ions and multiphoton ionization.

C. S. Feigerle (University of Tennessee, Department of Chemistry) received tenure and promotion from Assistant to Associated Professor.

Photoelectron angular distributions from resonantly enhanced multiphoton ionization of xenon via the $6s[3/2]_1^\circ$ and $6s'[1/2]_1^\circ$ states: experiment and theory

Perry R. Blazewicz

Department of Chemistry, Yale University, New Haven, Connecticut 06520

Xian Tang

Department of Physics, The University of Southern California, Los Angeles, California 90089-0484

Robert N. Compton and John A. D. Stockdale

Chemical Physics Section, Health and Safety Research Division, Oak Ridge National Laboratory, Oak Ridge, Tennessee 37831-6125

Received November 24, 1986; accepted January 13, 1987

Photoelectron energy and angular distributions are reported for resonantly enhanced multiphoton ionization (REMPI) through the three-photon-allowed $6s[3/2]_1^\circ$ and $6s'[1/2]_1^\circ$ states of xenon at laser-power densities of $\sim 10^9$–10^{11} W/cm^2. Ionization from three-photon resonance with the $6s[3/2]_1^\circ$ state gives two photoelectron peaks corresponding to leaving the ion in either the $^2P_{3/2}$ or the $^2P_{1/2}$ state. It is found that the two groups of photoelectrons have distinctly different angular distributions. Calculations indicate that configuration mixing in the 6*s* manifold is important in describing the observed angular distributions. REMPI via the $6s'[1/2]_1^\circ$ state gives one main photoelectron peak resulting from autoionization to the $^2P_{3/2}$ state of the ion. Two additional peaks of higher-energy photoelectrons are seen, which are due to the absorption of an additional photon before ionization. Strong core-changing processes are evident in the spectra.

INTRODUCTION

Measurements of photoelectron angular distributions resulting from multiphoton ionization (MPI) of atoms represent an active area of research.[1] When combined with theory, these studies provide much insight into the dynamics of the ionization process and the wave functions describing the intermediate and continuum states.[2]

Previous reports by Compton *et al.*[3] and Miller and Compton[4] have given the photoelectron energy spectrum for MPI resonantly enhanced via three-photon resonance with the xenon $6s[3/2]_1^\circ$ state. These have been followed by measurements by Kruit *et al.*[5] and by Sato *et al.*[6] of the angular distributions for the photoelectrons produced in this [3 + 2] ionization.

Here, we report a reinvestigation of these MPI photoelectron angular distributions and note features unseen in the previous reports. In addition, we report the first observation to our knowledge of photoelectron energy and angular distribution spectra from the corresponding MPI resonantly enhanced through the $6s'[1/2]_1^\circ$ state. These two resonant ionization processes yield different photoelectron angular distributions. The experimental results are compared with multichannel-quantum-defect theory (MQDT) calculations.

EXPERIMENT

A schematic diagram of the experimental apparatus is shown in Fig. 1. The output of a pulsed, amplified dye laser (Quanta-Ray PDL-2) pumped by a Nd:YAG laser (Quanta-Ray DCR) has its polarization purified by a Glan air prism and is focused into the vacuum chamber with a 50- or 38-mm focal-length lens to a power density of $\sim 10^9$–10^{11} W/cm^2. The laser beam crosses xenon atoms introduced into the vacuum chamber through a pulsed nozzle (Lasertechnics, Inc.). The gas jet from the nozzle is perpendicular to the laser beam and to the normal to the entrance face of the electrostatic energy analyzer. The analyzer has a 12.7-cm mean radius, twice the size of those previously employed in this laboratory.[3,4] This larger analyzer allows for higher resolution or greater throughput of electrons at a given resolution. The analyzer is operated in the fixed-pass energy mode. Photoelectrons selected by the analyzer are detected with a dual-microchannel plate detector, and the signal is preamplified, averaged with a boxcar averager (EG&G PAR) and recorded on an x–y plotter. The plane of polarization of the dye laser was rotated continuously with a double Fresnel rhomb driven by a stepping motor to obtain continuous angular distributions. MPI of xenon is studied through the $6s[3/2]_1^\circ$ state around 440.8 nm using the dye Coumarin 440 and through the $6s'[1/2]_1^\circ$ state at 388.6 nm using the dye LD390.

RESULTS AND DISCUSSION

Figure 2 shows the energy-level diagrams, together with a global picture of the photoelectron energy spectra and angular distributions, for resonantly enhanced multiphoton ion-

0740-3224/87/050770-05$02.00

Nuclear Instruments and Methods in Physics Research B24/25 (1987) 325-328
North-Holland, Amsterdam

AUTODETACHMENT SPECTROSCOPY OF METASTABLE NEGATIVE IONS

T.J. KVALE *, G.D. ALTON and R.N. COMPTON **
Oak Ridge National Laboratory, Oak Ridge, Tennessee 37831-6125, USA

J.S. THOMPSON and D.J. PEGG +
The University of Tennessee, Knoxville, Tennessee 37996, USA

This paper is a review of some of our recent measurements on the metastable negative ions, Be^- and He_2^-, using the technique of fast-beam autodetachment spectroscopy

1. Introduction

Negative ions are of considerable current interest for both theoretical and practical reasons We have developed an experimental technique - fast-beam autodetachment spectroscopy - which permits us to investigate the structure of *metastable* negative ions These ions are formed when an electron attaches itself to an atom or molecule in a metastable excited state to form a configuration in which the spins of all the active electrons are aligned Such spin-aligned states are metastable against autodetachment and if they are the lowest-lying state of a given multiplicity they are also metastable against radiative decay Eventually, such states relax via forbidden autodetachment processes with lifetimes typically $\sim 10^{-6}$ to 10^{-4} s In this paper we review some of our recent measurements on metastable Be and He_2^- ions [1,2]

The source of the metastable negative ions studied using this experimental technique is a fast moving and unidirectional beam produced by charge changing a beam of momentum-selected positive ions in an alkali vapor cell The metastable spin-aligned state is formed following the sequential capture of two electrons The $(1s2s2p)^4P$ state of He is perhaps the most familiar state of this type In addition to investigating He (^4P), we have successfully produced and studied analogous doubly-excited and spin-aligned states such as the $(1s^2 2s 2p^2)^4P$ [4] state in the atomic ion, Be^-, and the $(1s\sigma_g^2 1s\sigma_u 2s\sigma_g 2p\pi_u)^4\Pi_g$ state in the molecular ion, He_2^- by the use of the method of fast-beam autodetachment spectroscopy.

2. Experimental arrangement

The major components of the apparatus are shown in fig. 1. An accelerator is used to produce a positive ion beam of the desired kinetic energy. The beam energy is chosen to efficiently produce negative ions by a double-electron capture process in a lithium vapor charge-exchange cell through which the positive ion beam is passed following momentum analysis. The different charge state components in the beam emerging from the charge exchange cell are separated electrostatically and the negative ions are deflected by 10° into a beam line containing a gas cell, a spherical sector electrostatic energy analyzer, and a shielded Faraday cup The spatial separation between the charge-exchange cell and the electron spectrometer corresponded, at the beam energies used in these measurements, to a time delay of a few microseconds between the production of the metastable negative ion state and the detection of electrons from the autodetaching decay of the state This arrangement ensures that we are studying only those states that are metastable against both autodetachment and radiative decay The gas cell is used to produce, when needed, a high-pressure region just in front of the spectrometer for the purpose of collisionally stripping electrons from the negative ion beam The electron signal from the energy analyzer is stored in a CAMAC-based multichannel scalar data acquisition system Three pairs of mutually perpendicular Helmholtz coils are used to reduce stray magnetic fields in the vicinity of the electron spectrometer

* Present address Department of Physics and Astronomy, The University of Toledo, Toledo, Ohio 43606, USA
** Also with the Department of Chemistry The University of Tennessee, Knoxville, Tennessee 37996, USA
+ Also with the Physics Division Oak Ridge National Laboratory, Bld 5500, MS 377, PO Box X, Oak Ridge, Tennessee 37831, USA

0168-583X/87/$03 50 © Elsevier Science Publishers B V. (North-Holland Physics Publishing Division)

Evidence for a Stable Negative Ion of Calcium

D. J. Pegg[a] and J. S. Thompson
Department of Physics, The University of Tennessee, Knoxville, Tennessee 37996

and

R. N. Compton[b] and G. D. Alton
Oak Ridge National Laboratory, Oak Ridge, Tennessee 37831

(Received 31 August 1987)

We present experimental evidence for the existence of a stable Ca^- ion formed in the bound $4s^24p\ ^2P$ state. This result represents the first report of a stable negative ion for a group-II*A* element. The structure of Ca^- was determined by means of photoelectron detachment spectroscopy. The electron affinity of Ca was measured to be 0.043 ± 0.007 eV, which is in good agreement with a recent calculation.

PACS numbers: 32.80.Fb, 35.10.Hn

In this paper we report on the first experimental determination of the structure of the Ca^- ion. We show, using photoelectron detachment spectroscopy, that this ion is stably bound, being formed in the $4s^24p\ ^2P$ state. This result is unexpected since in the past it has been generally believed that negative ions of all the group-II*A* (alkaline earths) elements are unstable.[1,2] The $2s^22p\ ^2P$ state in Be^-, for example, has been shown to lie ≈ 0.5 eV above the ground state of Be.[3,4] Similarly, the $3s^23p\ ^2P$ state in Mg^- has been detected as a shape resonance in the electron-atom elastic-scattering cross section at ≈ 0.15 eV.[5]

The existence of the Ca^- ion has been known for some time. Heinicke *et al.*,[6] for example, extracted this ion from a cold-cathode Penning-discharge source and, on the basis of time-of-flight arguments, estimated a lower limit of ≈ 10 μs on its lifetime. The ion has also been produced in double electron-capture collisions between Ca^+ ions and alkali-metal vapors.[7,8] Calculations such as those of Kurtz and Jordan,[9] however, failed to predict a stable state for the Ca^- ion but a calculation by Bunge *et al.*[10] did predict a metastable state, the spin-aligned $4s4p^2\ ^4P$ state. Earlier, we made an unsuccessful search for the electrons that should have served as a signature of the autodetaching decay of this metastable state. We were successful, however, in identifying the $2s2p^2\ ^4P$ state at the lighter group-II*A* element, Be^-, in similar experiments.[11] Subsequently, it was shown by Beck[12] that the lifetimes of the levels associated with this metastable state in Ca^- were reduced to the subnanosecond range by the strength of the magnetic interactions that drive the autodetachment process. In our case the time delay between the production of the ions and their detection was a few microseconds. It thus became clear that metastable states such as the $4s4p^2\ ^4P$ state could not be responsible for the existence of the long-lived Ca^- ions observed in this experiment and earlier by Heinicke *et al.*[6] As a result we were led to conclude that the Ca^- ion was probably stable despite the lack of theoretical evidence at that time. In a recent calculation involving extensive correlation effects, Froese Fischer and co-workers[13] predicted that the $4s^24p\ ^2P$ state in the Ca^- ion is bound by 0.045 eV with respect to the ground state of the Ca atom.

The present photodetachment spectroscopy measurements were made with the crossed-beam apparatus shown schematically in Fig. 1. The overall apparatus is similar to that used in our earlier autodetachment measurements[11,14,15] and a previous photodetachment cross-section measurement.[16] A beam of Ca^- ions was produced by our passing Ca^+ ions in the energy range from 60 to 80 keV through a Li-vapor charge-exchange cell. A study of the production of Ca^- ions as a function of beam energy and Li target density has been reported by Alton *et al.*[8] Following a delay of a few microseconds, the beam leaving the charge-exchange cell was charge-state analyzed and the negative component was deflected through 10° into a beam line containing a spherical-sector electron energy analyzer. Just prior to the entrance of this analyzer the negative-ion beam was crossed perpendicularly with a photon beam from a linear flashlamp-pumped pulsed dye laser (Candela Corporation model LFDL-8). The laser was operated at a repetition rate of 10 Hz and the pulse duration was 2.2 μs. The linear polarization vector of the laser beam was aligned along the ion beam axis. The bandwidth of the laser was 2 Å. A 10-cm focal-length lens was used to focus the laser beam onto the ion beam. The lens produced a focal diameter of about 0.2 mm. The maximum laser power used in the experiment was ≈ 0.5 MW which produced a power density of $\approx 10^8$ W/cm^2 in the interaction region. The optical or ac Stark effect on a bound-continuum transition is known to be generally small (except for possible resonances in the continuum) at photoionization thresholds. Similarly, at photodetachment thresholds the cross sections are small and any

Autodetachment Spectroscopy of Metastable He_2^-

T. J. Kvale, R. N. Compton,[a] and G. D. Alton
Oak Ridge National Laboratory, Oak Ridge, Tennessee 37831

and

J. S. Thompson and D. J. Pegg[b]
The University of Tennessee, Knoxville, Tennessee 37996

(Received 8 November 1985)

Two distinct autodetachment channels are observed in the electron energy spectra of He_2^- formed by double charge exchange of energetic He_2^+ (30–65 keV) in lithium vapor. A single narrow peak has a center-of-mass energy of 11.5 ± 2.6 meV, and is attributed to vibrational autodetachment [e.g., $He_2^-(^4\Pi_g)_{v=1} \rightarrow He_2^0(a\,^3\Sigma_u^+)_{v=0} + e$]. A second broad peak has a center-of-mass energy of 15.78 ± 0.13 eV and results from autodetachment of He_2^- into the $He_2(X\,^1\Sigma_g^+) + e$ repulsive continuum. An electron affinity of 0.175 ± 0.032 eV was determined for the $^4He_2(a\,^3\Sigma_u^+)$ state by comparison of the $^3He_2^-$ and $^4He_2^-$ autodetachment spectra.

PACS numbers: 33.80.Eh, 35.20.Vf

There has been considerable recent interest in metastable negative ions. Atomic negative ions such as He^- (see Alton, Compton, and Pegg[1]), Be^- (see Bae and Peterson[2] and Kvale *et al.*[3]), and Li^- (see Brooks *et al.*[4]) have received the most attention. Particular attention has been devoted to theoretical studies of Feshbach resonances of atomic systems.[5] Long-lived ($\tau > 10^{-6}$ s) polyatomic negative ions are known to exist as electronically or nuclear excited Feshbach resonances[6] and lifetimes for many of these systems have been measured. Although a few metastable diatomic negative ions are known to exist, little is known about the energy levels and autodetachment lifetimes of these species. One notable exception is the study of the autodetachment of C_2^- by Hefter *et al.*[7]

In this note, we present the first experimental data on the structure of He_2^- obtained via autodetachment spectroscopy of a fast He_2^- negative-ion beam. Two very distinct autodetachment processes are observed, one involving vibrational autodetachment and a second process that we call "excimer autodetachment" which involves detachment into the $He(^1S) + He(^1S) + e$ continuum. The high resolution possible in the center-of-mass system for most light species (< 10 meV), along with the ability to study ultralow-energy electrons, establishes this technique as a powerful method of molecular spectroscopy.

Long-lived metastable negative-ion beams of He_2^- have recently been produced by Bae, Coggiola, and Peterson[8] by using double charge exchange of He_2^+ ions with cesium vapor. The electronic structure of He_2^- was subsequently investigated by Michels[9] who found the $He_2^-(^4\Pi_g)(1s\sigma_g^2 1s\sigma_u 2s\sigma_g 2p\pi_u)$ state to be bound relative to the lowest triplet state $He_2^*(a\,^3\Sigma_u^+)$ by 0.233 eV. These calculations further show that the $He_2^-\ ^4\Sigma_g^+(1s\sigma_g^2 1s\sigma_u 2s\sigma_g 2s\sigma_u)$ negative-ion state is unbound relative to the $He_2^*(a\,^3\Sigma_u^+)$ state for internuclear separations $\lesssim 6$ Å. For internuclear separations near the potential minimum (~ 1 Å), the $He_2^-\ ^4\Sigma_g^+$ state tracks sufficiently close to the $He_2^*(a\,^3\Sigma_u^+)$ state that it was not possible to determine whether this state is stable. More extensive calculations on this potential show that the $^4\Sigma_u^+$ state is unbound at all internuclear separations.[10] Bae, Coggiola, and Peterson[8] estimated autodetachment rates for He_2^- and observed some ions with lifetimes exceeding 10^{-4} s and others with lifetimes of less than 10^{-5} s. These authors point out the possibility of decay of an ensemble of metastable rovibronic states of He_2^-.

Experimental details can be found in previous publications.[1,3] Briefly, a He_2^+-ion beam formed in a hollow-cathode positive-ion source was accelerated to 30–65 keV and momentum analyzed by a 90° bending magnet. The He_2^+-ion beam was then focused through a lithium-vapor charge-exchange cell located 3 m from the bending magnet and $\frac{1}{4}$ m from the electron spectrometer. The positive, negative, and neutral particles emergent from the lithium-vapor cell were electrostatically separated upon entrance into the experimental chamber. He_2^- ions passing into the chamber were deflected by 10° into the electron spectrometer. The electrostatic charge-state separation system was also effective in eliminating lower-energy ion-beam fragments which could be produced by collisional processes. By adjustment of the deflector potential, a lower-intensity He^- ($^4P^o$) beam, resulting from the breakup of He_2^+ in collisions with lithium, was also observed. The autodetachment spectrum for this beam was identical to that reported for He^- ($^4P^o$) previously[1] and was used to estimate the electron energy resolution of the spectrometer. Electrons ejected in the forward and backward directions from the motion of the ion beam were energy analyzed by a 160°

Photoelectron Angular Distributions for Near-Threshold Two-Photon Ionization of Cesium and Rubidium Atoms

Adila Dodhy
Physics Department, Auburn University, Auburn, Alabama 36849, and Oak Ridge National Laboratory, Oak Ridge, Tennessee 37831

and

R. N. Compton and J. A. D. Stockdale
Chemical Physics Section, Health and Safety Research Division, Oak Ridge National Laboratory, Oak Ridge, Tennessee 37831

(Received 1 October 1984)

Photoelectron angular distributions have been measured for nonresonant two-photon ionization of cesium and rubidium atoms just above the ionization threshold. The photoelectron energies ranged from 25 to 100 meV. The results are compared with theoretical estimates based on nonrelativistic atomic wave functions. Initial results are also presented for above-threshold ionization in cesium.

PACS numbers: 32.80.Fb, 32.80.Rm

Multiphoton ionization (MPI) of atoms promises new insights into various problems of atomic structure and dynamics.[1-3] Perhaps the most powerful approach is the measurement of differential cross sections,[4-10] where the angular distributions of the photoejected electrons provide data not only on the magnitudes of the transition amplitudes but also on their relative phases. In addition to providing information about the scattering phase, thus complementing single-photon studies,[11] such measurements also test our theoretical understanding of high-order bound-free transitions involving sums over virtual intermediate states.[12]

Studies of photoelectron angular distributions for alkali-metal atoms have been limited to cases of resonantly enhanced MPI[4-6,8,10] or higher-order nonresonant processes.[7,12,13] In this paper, we report photoelectron angular distributions for nonresonant two-photon ionization of cesium and rubidium atoms where the photoejected electron has an energy in the range ~25–100 meV. Figure 1 shows the ionization scheme for both alkali metals. The first photon lies between the $6p$ and $7p$ states for cesium and between the $5p$ and $6p$ states for rubidium.

Our measurements are novel in two respects. First, we have studied photoelectron angular distributions in a region very close to the ionization threshold. This is difficult experimentally because of the very low energy of the photoelectrons under consideration. Second, we report photoelectron angular distributions for above-threshold ionization of cesium and compare them with theoretical predictions. Such processes have been observed by others in xenon[14-18] and cesium[13] but only in higher order (order 5 in cesium and ≥ 6 in xenon).

Details of the experimental apparatus have been described recently[10] in conjunction with resonantly enhanced MPI. Briefly, the output from a Nd:YAlG (yttrium aluminum garnet) pumped dye laser (Quanta Ray, DCR-II, PDL-I) was crossed orthogonally by a thermal alkali-metal beam. The dye-laser pulse duration was 5 ns and the bandwidth was 0.02 nm. The laser was focused to a power density of 10^8 W/cm^2 by a 35-mm lens. The power density was an order of magnitude greater when electrons from above-threshold ionization were studied. The plane of polarization of the laser was rotated by a double-Fresnel rhomb. Photoelectrons emerging perpendicular to the propagation vector of the laser beam and within $\pm 2°$ were energy analyzed by a 160° spherical-sector electrostatic energy analyzer. They were then detected by

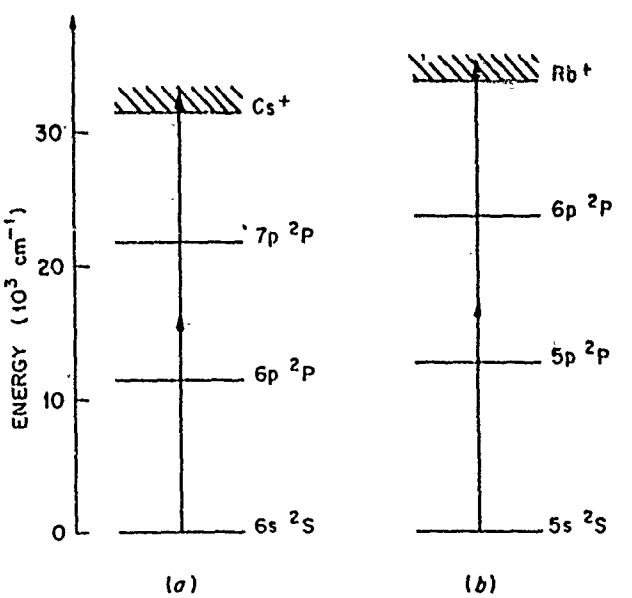

FIG. 1. Energy-level diagram showing the excitation scheme leading to ionization for nonresonant two-photon ionization of (a) cesium atoms and (b) rubidium atoms.

Experimental Determination of the Energy Level of $Be^-(1s^22s2p^2)^4P$

T. J. Kvale, G. D. Alton, and R. N. Compton[a]
Oak Ridge National Laboratory, Oak Ridge, Tennessee 37831

and

D. J. Pegg[b] and J. S. Thompson
The University of Tennessee, Knoxville, Tennessee 37996

(Received 11 March 1985)

We report the first experimental measurements for the energy level of a metastable state of Be^-. The ions were produced in sequential charge-exchange collisions between 50- to 60-keV Be^+ ions and lithium vapor. The center-of-mass energy of autodetaching electrons was found to be 2.53 ± 0.09 eV. This result is in good agreement with previously calculated values for the $Be^-(1s^22s2p^2)^4P$-state energy.

PACS numbers: 32.80.Dz, 35.10.Hn

In this paper, we report the observation of a peak in the Be^- autodetachment electron-energy spectrum which is a signature of the decay of a metastable beryllium negative-ion state. These measurements represent the first time that the energy level of a long-lived metastable state has been experimentally determined for negative ions of the group IIA (alkaline-earth) elements. In fact, limited experimental information is available on the structure of any metastably bound atomic negative ion. Notable exceptions to this include He^-, which is a classic example of a spin-aligned metastable negative ion (see, e.g., Alton, Compton, and Pegg[1]); resonance studies from electron-atom scattering experiments (see, e.g., Burrow, Michejda, and Comer[2]); and Li^-, in which photon emission was observed between high-lying metastable states of the negative ion (see, e.g., Brooks *et al.*[3]). The fundamental nature of Be^- makes it of considerable experimental and theoretical interest. As early as 1966, the ion was reported[4,5] to be present in mass spectra of ions emitted from direct-extraction negative-ion sources. Since the first observation of Be^-, experimental values for production efficiencies[6] and autodetachment lifetimes[7] have been reported. In recent measurements on the autodetaching decay of Be^-, Bae and Peterson[7] have shown that the ion has at least two distinct lifetime components of $\sim 10^{-4}$ and $\sim 10^{-5}$ s.

Most theoretical studies indicate that Be^- is metastable,[8-13] although early theoretical calculations[14-16] suggest that $Be^-(1s^22s^23s)^2S$ is bound with respect to the ground state, $(1s^22s^2)^1S$, of beryllium. Recent theoretical calculations do not predict the existence of a stable Be^- state but predict the existence of two states, both metastable against autodetachment, which lie below the first ionization threshold of neutral beryllium—$Be^-(1s^22s2p^2)^4P$ which is bound with respect to $Be(1s^22s2p)^3P^\circ$, and $Be^-(1s^22p^3)^4S^\circ$ which is bound with respect to $Be(1s^22p^2)^3P$. The radiatively allowed $^4S^\circ \rightarrow {}^4P$ transition is predicted to occur at either 263.8 nm (Ref. 9), 267.1 nm (Ref. 12), or 265.4 nm (Ref. 10). Radiation from this transition was searched for by Andersen[17] without success. A third metastable state, $Be^-(1s2s2p^3)^6S^\circ$, has also been predicted.[9,12] This state, however, lies energetically outside the present experimental range [≥ 100 eV from $Be(1s^22s^2)^1S$]. Other Be^- ion states have also been theoretically studied. For instance, the $Be^-(1s^22s^22p)^2P$ configuration is predicted[18] to be a shape resonance; however, the lifetime of this state is too short to be studied with the present apparatus.

Theoretical calculations of the structure of negative ions are particularly difficult since the electron affinities are typically of the same magnitude as the difference in correlation energies between the atom and ion. Even so, most of the present information concerning metastable negative ions, other than He^-, has been provided by theoretical studies of open-shell excited-state negative-ion configurations. The first theoretical investigations of the structure and binding energies (electron affinities) for the group IA elements Li^-, Na^-, and K^- and the group IIA elements Be^- and Mg^- were made by Weiss[8] who employed variational-superposition techniques. The Be^- ion was predicted to be bound relative to the neutral atomic $(1s^22s2p)^3P^\circ$ state by 240 meV with the most likely configuration postulated to be $Be^-(1s^22s2p^2)^4P$. This configuration is metastable against autodetachment by spin-forbidden transitions—analogous to the $(1s2s2p)^4P^\circ$ state of He^-.

Configuration-interaction calculations have been employed by Bunge *et al.*[9] in a search for possible bound excited negative-ion state configurations for the elements hydrogen through calcium. The results of these investigations indicate the existence of two metastable states of Be^-—the $Be^-(1s^22s2p^2)^4P$ which is bound relative to $Be(1s^22s2p)^3P$ by 285 meV, and $Be^-(1s^22p^3)^4S^\circ$ which is bound relative to the $(1s^22p^2)^3P$ atomic state by 262 meV.

The fine and hyperfine energy separations, as well as

High-order multiphoton ionization photoelectron spectroscopy of nitric oxide[a)]

H. S. Carman, Jr. and R. N. Compton
Chemical Physics Section, Health and Safety Research Division, Oak Ridge National Laboratory, Oak Ridge, Tennessee 37831-6125 and Department of Chemistry, The University of Tennessee, Knoxville, Tennessee 37996

(Received 3 October 1988; accepted 26 October 1988)

Resonance-enhanced and nonresonant five- and six-photon ionization of NO was studied using angle resolved photoelectron spectroscopy. The (3 + 3) resonance-enhanced multiphoton ionization photoelectron spectrum (REMPI-PES) of NO via the $A\,^2\Sigma^+$ ($v=0$) level yielded a distribution of electron energies corresponding to all accessible vibrational levels ($v^+ = 0$–6) of the nascent ion. The observed energy distributions suggest near resonant enhancement due to vibrational levels of the $D\,^2\Sigma^+$ and $C\,^2\Pi$ states at the fourth photon level. Angular distributions of photoelectrons corresponding to $v^+ = 0$ and $v^+ = 3$ (rotationally unresolved) were significantly different, perhaps reflecting these different pathways. The (3 + 2) REMPI via the $A\,^2\Sigma^+$ ($v=1$) level produced only one low-energy electron peak corresponding to $v^+ = 1$. Nonresonant MPI at 532 nm yielded a distribution of photoelectron energies corresponding to both four- and five-photon ionization. Prominent peaks in the five-photon ionization photoelectron spectrum show that near resonant enhancement occurs via the $A\,^2\Sigma^+$ ($v=5$), the $C\,^2\Pi(v=2)$ and the $D\,^2\Sigma^+$ ($v=1$) states at the three-photon level. This study amply demonstrates the utility of angle resolved MPI-PES in understanding high-order multiphoton ionization processes. Finally, measurements of the ratio of NO^+ ion signal for circular and linear polarized light when tuning near the $A\,^2\Sigma^+$ ($v=0$) and $A\,^2\Sigma^+$ ($v=1$) levels are reported and compared with theory.

INTRODUCTION

Resonance-enhanced multiphoton ionization photoelectron spectroscopy (REMPI-PES) has become an established tool for probing the photoionization dynamics of atoms and molecules.[1,2] In principle, measurements of photoelectron angular distributions (PEADs) in a REMPI process can provide information about both the dynamics of the bound–continuum transition and the alignment of an optically prepared intermediate state.[3] To date, MPI-PES studies of diatomic molecules have included only a half-dozen or so molecules (H_2, N_2, O_2, CH, CO, NO, I_2, Br_2, and Cl_2). Of these, NO has received the major attention due to its low ionization potential and rich electronic structure. MPI-PES studies have been reported for approximately sixteen electronically excited states of NO (see Ref. 2).

The one-photon absorption spectrum of NO is very complex and consists of intense Rydberg series and long vibrational progressions of valence states. Jungen[4] has used such spectra to show that the single ground state valence electron can be closely represented as a united atom $3d\pi$ electron with a small $2p\pi$ admixture. Consequently, the intensities of one-photon np and nf Rydberg series are much larger than the ns and nd series. As a result of the mixed character of the ground state, multiphoton transitions to upper Rydberg states are allowed for all even or odd numbers of photons. The pioneering studies of Johnson and coworkers[5] have amply illustrated this property of NO. The $A\,^2\Sigma^+$ state is the lowest member of the Rydberg series converging to the ground ionic state, and numerous REMPI-PES studies have been performed for the case of (1 + 1) and (2 + 2) REMPI-PES. In this paper we report the first study of (3 + 3) and (3 + 2) REMPI via the $A\,^2\Sigma^+$ state.

EXPERIMENTAL

The apparatus and experimental techniques have been described previously[6] and will only be briefly mentioned here for completeness. The laser beams used in these studies consisted of: (1) the frequency-doubled output (532 nm) of the fundamental (1.06 μ) of a Quanta Ray DCR II Nd:YAG oscillator amplifier and (2) the tunable output from a Quanta-Ray PDL-2 dye laser operating with LDS 698 dye for $A\,^2\Sigma^+$ ($v=0$) studies and DCM for $A\,^2\Sigma^+$ ($v=1$) studies. In both cases the laser beam was focused by a 50 mm focal length lens to a peak power density of $\sim 10^9$ W/cm^2. The beam was focused into a pulsed, supersonic jet of neat NO gas directly in front of the entrance aperture of a 7 cm radius spherical sector electrostatic energy analyzer operating with a theoretical resolution of ~0.02 eV. However, due to space charge effects and possible laser power broadening, the resolution is ~0.15 eV. Although the actual electron signal was low in these studies compared with similar data for (1 + 1) or (2 + 2), REMPI via the $A\,^2\Sigma^+$ state, the relatively poor electron energy resolution is probably reflective of the fact that most of the signal originates during

[a)] Research sponsored by the Office of Health and Environmental Research, U.S. Department of Energy under Contract No. DE-AC05-84OR21400 with Martin Marietta Energy Systems, Inc.

the high intensity "spikes" known to occur during the laser pulse duration. The actual signal was averaged over ~10 laser flashes. In order to observe and record signal, it was imperative to operate the laser at its maximum intensity. It was also necessary to maintain fresh dye solution in the dye laser in order to optimize the output.

NO^+ ions could also be observed using a ~20 cm time-of-flight mass spectrometer. A Tektronix digital oscilloscope was used to record the TOF spectra. Under the conditions of our nozzle expansion, moderate cooling was occurring. This proved relatively unimportant due to the extreme line broadening observed in the wavelength-resolved spectra at the power densities employed.

Studies of REMPI of NO comparing circularly polarized light with linearly polarized light were carried out using a Soleil-Babinet compensator to obtain the desired polarization. For the angular distribution measurements, a double Fresnel rhomb polarization rotator was used.

RESULTS AND DISCUSSION

Multiphoton ionization photoelectron spectroscopy using linearly polarized light

Figure 1 depicts the various four-, five-, and six-photon ionization processes studied in this work along with some of the states involved. The dependence of the NO^+ signal as a function of wavelength for six photon ionization of NO in the region where three photons are in near resonance with the $A\,^2\Sigma^+$ ($v = 0$) state is shown at various laser powers in Fig. 2. Even at the lowest power, the spectra show no rotationally resolved states but rather a broad continuum which

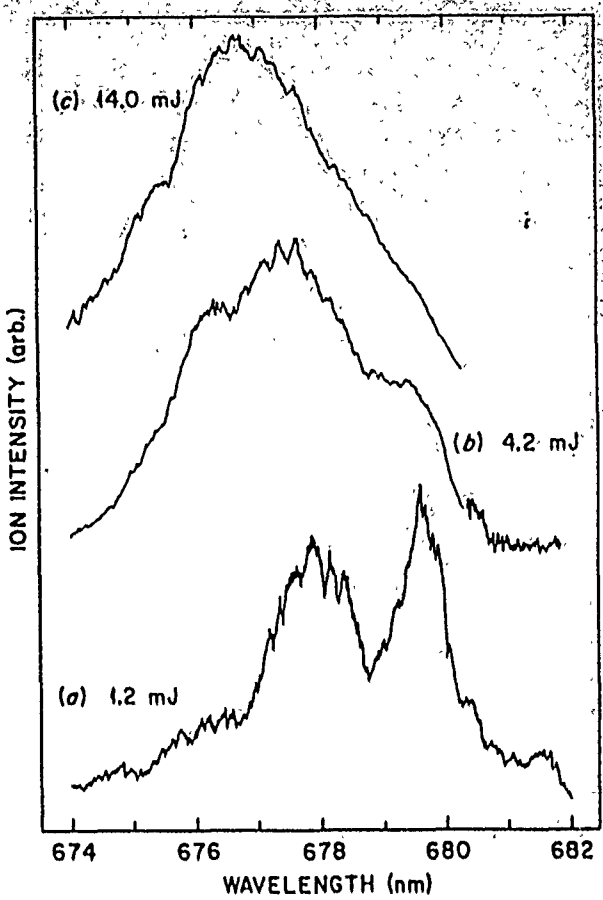

FIG. 2. Laser power dependence of the NO^+ ion signal observed when tuning the laser wavelength near the three-photon allowed $A\,^2\Sigma^+$ ($v = 0$) state. Similar spectra were recorded when tuning near the three-photon allowed $A\,^2\Sigma^+$ ($v = 1$) state near 645 nm (laser wavelength).

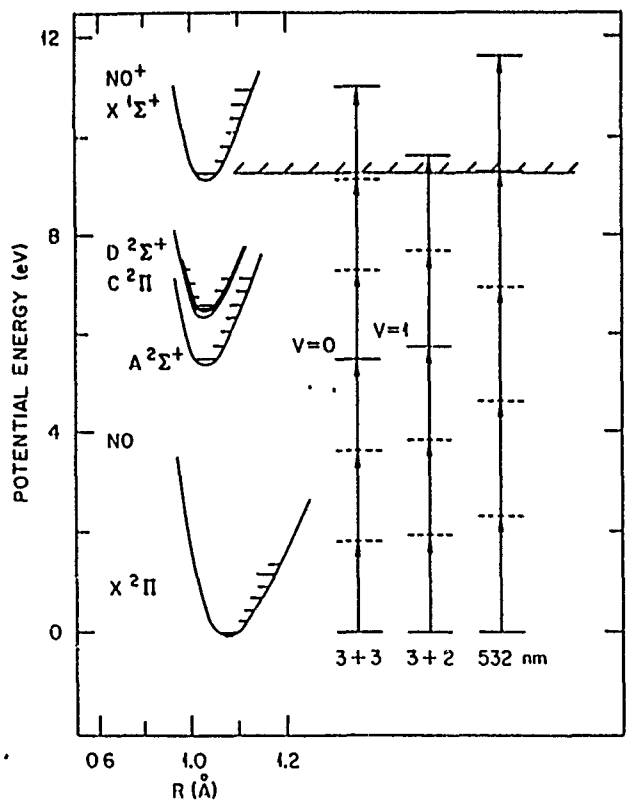

FIG. 1. Illustration of the five- and six-photon multiphoton ionization processes studied in this paper

shifts to shorter wavelength as the laser power increases. Very similar, broad spectra, were recorded at the $A\,^2\Sigma^+$ ($v = 1$) state.

For purposes of discussion, the generalized N-photon ionization rate can be written using the lowest order time-dependent perturbation theory as:

$$R = \hat{\sigma}_N F^N , \tag{1}$$

where σ_N is the generalized N-photon ionization cross section with units of $cm^{2N}\,sec^N$ and F is the photon flux in units of photons $cm^{-2}\,s^{-1}$. $\hat{\sigma}_N$ is obtained by first calculating a summation of all the matrix elements coupling the ground state to the continuum over all of the possible resonant intermediate states divided by the detuning of the N photons with each energy level. This complicated sum is then squared to obtain $\hat{\sigma}_N$. In addition, the ground and excited state energy levels of a molecule will shift in the presence of electromagnetic radiation as a result of the ac Stark effect. In general, the shift of a particular level k depends upon the energy of all other levels and can be approximated by first-order perturbation theory as

$$S_k = \sum_{l \neq k} \frac{|V_{kl}|^2}{\omega_k - \omega_l + \omega} + \sum_{l \neq k} \frac{|V_{kl}|^2}{\omega_k - \omega_l - \omega}, \tag{2}$$

where V_{kl} is the component of the Hamiltonian coupling state l and k. The ac Stark effect coupled with possible satu-

ration effects at the three-photon level are assumed to account for the broadening and shifting of the REMPI spectra shown in Fig. 2. The many photons involved in the present study coupled with the resonance involved at the three-photon level, the near resonances at the four- and five-photon levels, and the known autoionization structure at the continuum six-photon level makes a theoretical analysis of this problem [solution of Eq. (1), subject to Eq. (2)] a formidable task. Zakheim and Johnson[5] used Eq. (1) to discuss the problem of (2 + 2) and (3 + 1) REMPI of NO where one resonance and other near resonances were involved. They argued that this treatment predicts that $\hat{\sigma}_v$ for both process would be of comparable magnitudes whereas the experimentally observed MPI signal for the $A\,^2\Sigma^+, 3s\sigma$ state is at least two orders of magnitude larger than any three-photon resonance. They concluded that "a kinetic rate equation description provides a basic framework for the interpretation of multiphoton ionization spectra initiated by a pulsed, multimode dye laser."

The fact that the observed wavelength spectra are broad and rotationally unresolved both simplifies and complicates the analysis of the data presented. Since there is no rotational structure, angular distributions were only recorded over the width of the broad structure, not for different rotational states. It is important to note here that the photoelectron angular distributions and the measurements of linear to circular polarized light ratios were relatively insensitive to tuning within the Stark shifted profile.

Figure 3 shows a representative photoelectron spectrum (PES) obtained for (3 + 3) REMPI via the $v = 0$ level of the $A\,^2\Sigma^+$ state at 676.2 nm (laser power ~ 14 mJ). The basic overall spectrum did not change when tuning to other wavelengths within the resonance, although the peak heights varied and at some wavelengths $v^+ = 2$ and 4 appeared. Due to the Rydberg character of the $A\,^2\Sigma^+$ state, the Franck–Condon principle predicts that direct ionization of the $v = 0$ level would produce only the $v^+ = 0$ level of the ion with observable intensity. Although $v^+ = 0$ is the strongest member of the series, the appearance of higher v^+ levels of NO^+ thus suggests the contribution of additional ionization mechanisms, as discussed previously for (2 + 2) and (1 + 1) processes.[2,7] The occurrence of ~0 eV electrons has been discussed by many authors (see Ref. 2) for (1 + 1) and (2 + 2) REMPI and has been ascribed to autoionization and/or Rydberg–valence mixing. Such slow electrons have been observed in one-photon ionization as well.[8] In the previous studies of (1 + 1) or (2 + 2) REMPI it was not possible to solely implicate states at the three-photon level. In the present case, the four-photon level is near the low vibrational members of the $C\,^2\Pi$ and $D\,^2\Sigma^+$ states, and we can directly observe their influence on the PES. Close inspection of Fig. 1 shows that the fourth photon for the (3 + 3) process via the $A\,^2\Sigma^+$ ($v^+ = 0$) state is in near resonance with the $v = 3$ level of the C state. The fourth photon is also in near resonance with the $v = 7$ level of the $A\,^2\Sigma^+$ state and $v = 3$ of $D\,^2\Sigma^+$ state. Such resonances are expected to play some role in the occurrence of $v^+ = 6$ and 5. Possible mixing at the fifth photon level might complicate the dynamics further. Thus the occurrence of $v^+ = 0$ and $v^+ = 3$ are ascribed to near resonances of the third and fourth photon with the $A\,^2\Sigma^+$ ($v = 0$) and $C\,^2\Pi$ ($v = 3$) levels, respectively.

Photoelectron angular distributions, PEADs, were determined for electrons corresponding to $v^+ = 0$ and 3 and are shown in Fig. 4. Figure 5 shows a typical angular distribution measurement (for $v^+ = 0$) illustrating the quality of the data representing measurements as a function of angle for $\theta = 0$ to 2π. Each angular distribution measurement

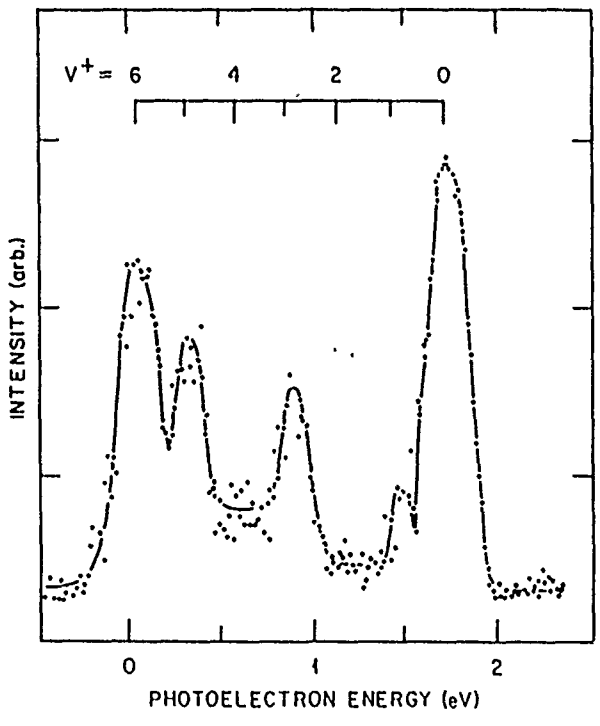

FIG. 3. Multiphoton ionization photoelectron spectrum MPI-PES of NO when tuning the laser at 676.2 nm (see Fig. 2) such that the $A\,^2\Sigma^+$ ($v = 0$) level is near the three-photon excitation region. Laser power is ~14 mJ/pulse

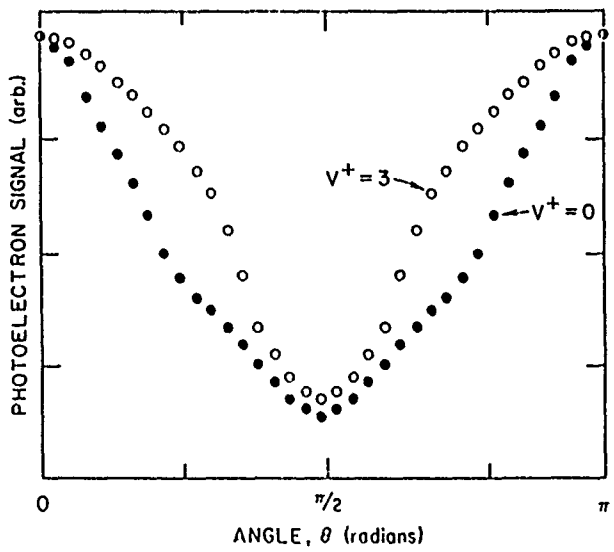

FIG. 4. Photoelectron angular distributions for photoelectrons corresponding to leaving NO^+ in the $v^+ = 3$ and $v^+ = 0$ states following six-photon ionization of NO

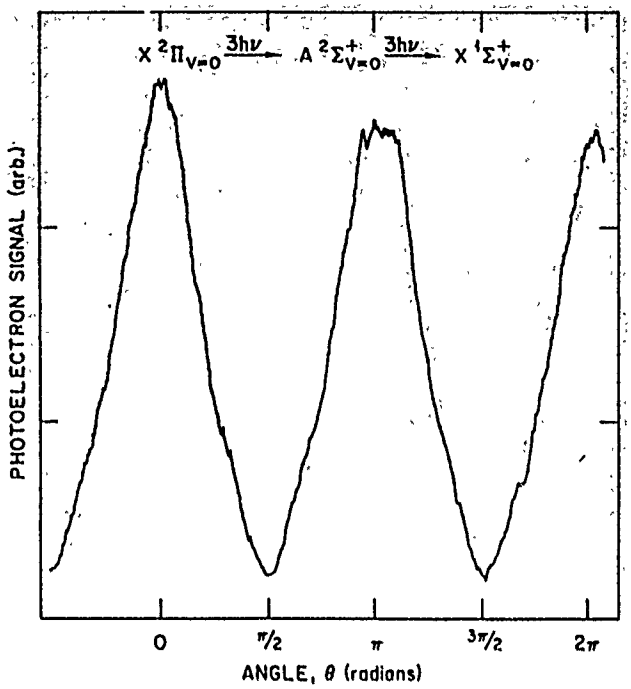

FIG. 5. Representative measurements of the angular distributions for six-photon ionization of NO leaving the NO^+ ion in the $v^+ = 0$ level.

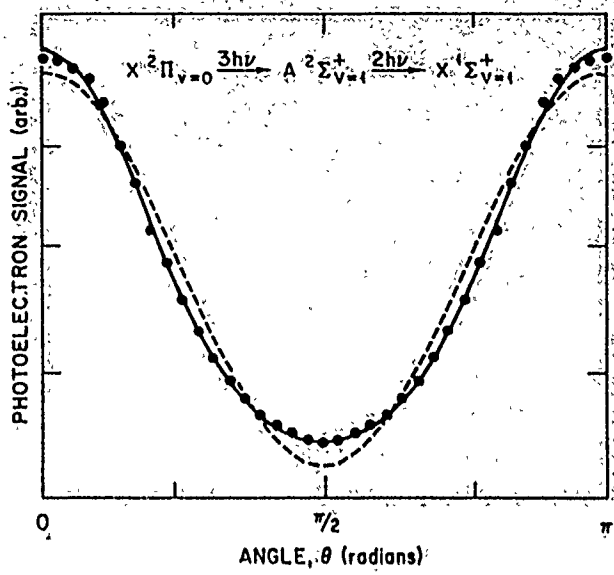

FIG. 6. Photoelectron angular distributions for (3 + 2) REMPI via the $A\,^2\Sigma^+$ ($v = 1$) state. The solid line represents Eq. (6) and the dashed line is an attempt to fit to only $P_2(\cos\theta)$.

$\theta = 0$ to 2π took about 5 min. The signal slowly falls off as a result of degradation of the laser dye. The point by point data shown in Fig. 4 represents the average of many such distributions. The angular distributions shown in Fig. 4 were fit using a least-squares procedure, to a Legendre polynomial expansion

$$I(\theta) = \sum_{k=0}^{N} \alpha_{2k} P_{2k}(\cos\theta), \tag{3}$$

where N is the order of the ionization process. It was found that inclusion of terms up to $P_6(\cos\theta)$ were necessary to fit the data:

$v^+ = 0$:

$$I(\theta) = 1 + 1.23(1)P_2 + 0.16(2)P_4 + 0.22(3)P_6, \tag{4}$$

$v^+ = 3$:

$$I(\theta) = 1 + 1.07(1)P_2 - 0.34(1)P_4 + 0.13(1)P_6, \tag{5}$$

where uncertainties of the fit are shown in parentheses. This contrasts with recent (1 + 1) PEAD measurements via the $A\,^2\Sigma^+$ ($v = 0$) level for which the data were fit by including only the P_2 term.[9] Earlier measurements of the (2 + 2) angular distribution did require terms of order P_4 and P_6.[10] In the present experiments, terms up to order 12 are possible although only terms up to P_6 were necessary. The most dramatic difference between the distributions in Fig. 4 is the sign of the P_4 coefficients. Further theoretical investigation is necessary to determine if this difference might lead to a better understanding of the ionization mechanisms involved. Our data indicate that one ($v^+ = 0$) is a (3 + 3) REMPI process and the other ($v^+ = 3$) is a (4 + 2) REMPI process.

The (3 + 2) REMPI of the $A\,^2\Sigma^+$ ($v = 1$) level at 644.1 nm produced only one electron peak corresponding to $v^+ = 1$, indicating direct ionization. In this case the fifth photon is only slightly above the $v^+ = 1$ threshold, and channels leading to higher vibrational levels of the ion are not accessible. In order to fit the PEAD, it was necessary to include terms up to $P_4(\cos\theta)$:

$$I(\theta) = 1 + 1.54(2)P_2 + 0.32(2)P_4. \tag{6}$$

Figure 6 shows the measured PEAD along with a fit to only $P_2(\cos\theta)$ terms (dashed line). The solid line is the fit of Eq. (6). Unlike the case of (3 + 3) via the $A\,^2\Sigma^+$, the PEADs are almost represented by a simple $\cos^2\theta$ distribution.

We have also recorded a nonresonant MPI-PES spectrum of NO using the second harmonic of the Nd:YAG laser. In addition to studying the basic processes involved, it was felt that such a spectrum would be useful as a calibration spectrum for future MPI studies. Figure 7 shows the PES resulting from "nonresonant" MPI at 532 nm. We use the term nonresonant in quotations because the PES reflects near resonant contributions of upper states. Four photons are sufficient to ionize NO at this wavelength (0.06 eV above the $v^+ = 0$ threshold, see Fig. 1), and a very intense low energy electron peak is seen in the PES. In addition, several weaker peaks are observed at energies consistent with absorption of five photons, leaving the ion predominantly in the $v^+ = 1$, 2, and 5 vibrational levels. We note in Fig. 1 that the third photon energy is within ~800 cm^{-1} of the $A\,^2\Sigma^+$ ($v = 5$) $C\,^2\pi$ ($v = 2$) and $D\,^2\Sigma^+$ ($v = 1$) levels of NO. The MPI-PES clearly shows the importance of these resonances in the overall ionization mechanism.

Multiphoton ionization using both linearly and circularly polarized light

A Soleil-Babinet compensator was used to continuously change the polarization of the laser beam from linearly to elliptically to circularly polarized light. The purity of the circularly polarized light was determined to be greater than 98% (difference in the major to minor axis was less than 2%). The effects to be reported here are too large, and the

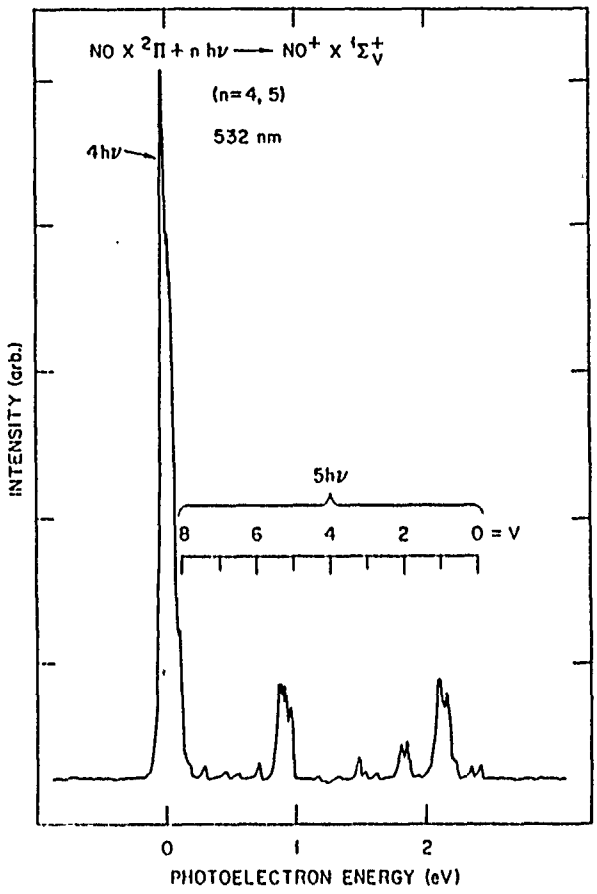

FIG. 7. Four- and five-photon ionization photoelectron spectrum of NO using the second harmonic (532 nm) of the Nd:YAG laser

error bars significantly great that such uncertainties in polarization are of no consequence in the measurements.

For the case of (3 + 3) REMPI via the $A\,^2\Sigma^+$ ($v = 0$) state, the ratio of NO^+ ion signal for circular light to linear light (σ_c/σ_l) was determined to be 0.34 ± 0.1. This measurement was determined at $\lambda = 676.16$ nm at a power of 14 mJ/pulse (see Fig. 2). However, no detectable difference was obtained at other power levels or wavelengths within the ac Stark shifted levels.

The ratio of signal for circularly polarized light to linearly polarized light for (3 + 2) REMPI via the $A\,^2\Sigma^+$ ($v = 1$) state was determined to be 0.11 ± 0.05. Thus, the ratio σ_c/σ_l for the (3 + 3) REMPI via the $v = 0$ level of the A state is approximately three times larger than that from the (3 + 2) process via the $v = 1$ level. More interestingly, σ_c/σ_l for both cases is considerably less than one.

Lowest-order perturbation theory has been employed to examine the question of the ratio (σ_c/σ_l) for low order N and low power laser MPI. (See, e.g., Ref. 11.) In these studies the maximum values obtained for $N = 3$ was 5/2 and for $N = 2$ was 3/2. Klarsfeld and Maquet[11] obtained a general prediction for N-photon ionization at low order:

$$\sigma_c/\sigma_l \leq \frac{(2N-1)!!}{N!}. \tag{7}$$

Equation (7) reduces to 3/2 for $N = 2$ and 5/2 for $N = 3$. These results have been obtained from lowest order perturbation theory and are only appropriate for low laser intensities and/or large detunings from resonance. There are a number of cases where σ_c/σ_l have been measured for low order ($N < 3$) MPI for atoms. The difficulties in treating the case of two-photon ionization of cesium atoms via a quadrupole transition at various laser powers has been treated recently both theoretically and experimentally[13] and illustrates the complexities involved. Further examples are also provided in Ref. 13.

We note that for low values of N, σ_c is greater than σ_l. This represents the fact that for low order the transition into the continuum for linearly polarized light can have two possible contributions $\Delta l = \pm 1$ which under proper conditions may interfere with one another, making σ_c (where Δl can be only +1 or -1) larger than σ_l. This presupposes that the pathway via the $N - 1$ levels are equivalent. For higher order (larger N) this will no longer be the case.

Reiss[14] has shown that previous[12] calculations for σ_c/σ_l for low order are misleading. Specifically, for MPI beginning with an S state (e.g., alkali) the number of final states possible for circularly polarized light is equal to l, while for linearly polarized light there are $\frac{1}{2}N + 1$ final states if N is even and $\frac{1}{2}(N + 1)$ if N is odd. In some cases $N = l$ may be the least important of the many allowed states in the linearly polarization case. Thus, σ_l will more likely be larger than σ_c for large N. In addition, even for low N, Dixit[15] has shown that because of the ac Stark effect at strong driving fields the maximum value of σ_c/σ_l can be much larger than $(2N-1)!!/N!$ near allowed resonances. As an example, for (2 + 1) REMPI via the $9D$ state in cesium, Dixit found that σ_c/σ_l approaches 50 near resonance.[15]

An actual calculation of the ratio of σ_c/σ_l to fit a given experiment is a complicated and difficult task requiring knowledge of the laser intensity, pulse duration, etc. Even for low order the difficulties are formidable (see Ref. 13) and outside the scope of this paper. It is instructive, however, to compare our results with the prediction of Reiss[14] of the upper bound for σ_c/σ_l for large order, N. He showed[14] that an upper bound on σ_c/σ_l can be approximated as

$$\frac{\sigma_c}{\sigma_l} = \frac{|R_c|^2}{|R_l|^2}\frac{A_c^2}{A_l^2}, \tag{8}$$

where the A's represent integrals over the angular function involving Clebsch–Gordon coefficients and the R's represent integrals over the initial- and final-state radial wave functions. A simplifying reduction of these integrals for large N can be written[14]

$$\frac{\sigma_c}{\sigma_l} \cong \frac{(N+1)(N+1)!}{(2N+1)!!}\frac{16}{e^2(2N^3)^{1/2}}\left(\frac{2e}{N}\right)^{2N}. \tag{9}$$

For $N = 6$, Eq. (9) gives $\sigma_c/\sigma_l = 0.008$; for $N = 5$, $\sigma_c/\sigma_l \simeq 0.131$. Although the result for $N = 5$ agrees with our measurements for (3 + 2) REMPI via the $A\,^2\Sigma^+$ ($v = 1$) state, the experimental result for (3 + 3) REMPI via the $A\,^2\Sigma^+$ ($v = 1$) state is a factor of 40 larger than the upper limit provided by Eq. (5). Thus, it is clear that more high-order MPI studies, both experimental and theoretical, for this and other (perhaps simpler) systems are needed. Our studies do, however, support the notion that σ_c will be smaller than σ_l for high order MPI processes as a result of the higher density

of allowed states available for linearly polarized light in comparison with circularly polarized light. More detailed studies will provide a tool for the analysis of higher order MPI as it has for low order. Comparison of photoelectron spectra for circular and linear polarized light may also afford further insight into the participation and nature of near resonances in MPI. In the present case, the low signals observed for circularly polarized light would not allow for measurement of photoelectron spectra of high enough quality in order to make such comparisons.

CONCLUSION

We have presented the first measurements of angle resolved photoelectron spectra for high order multiphoton ionization of a molecule (NO). The results clearly show the importance of resonant and near resonant enhancement in determining the overall multiphoton ionization processes involved. In addition, measurements of the ratio for circular to linear polarized light are reported and compared with existing theoretical notions.

ACKNOWLEDGMENTS

Research sponsored by the Office of Health and Environmental Research, U.S. Department of Energy under Contract No. DE-AC05-84OR21400 with Martin Marietta Energy Systems, Inc. H. S. C., Jr. acknowledges support from the U.S. Office of Naval Research Grant No. ONR393-071.

[1] K. Kimura, Adv. Chem. Phys. 60, 161 (1985).
[2] R. N. Compton and J. C. Miller, in *Laser Applications in Physical Chemistry*, edited by D. K. Evans (Marcel Dekker, New York, in press).
[3] S. N. Dixit and P. Lambropoulos, Phys. Rev. A 27, 861 (1983); S. N. Dixit, D. L. Lynch, and V. McKoy, in *Multiphoton Processes*, edited by P. Lambropoulos and S. J. Smith (Springer, New York, 1984); S. N. Dixit and V. McKoy, J. Chem. Phys. 82, 3546 (1985).
[4] Ch. Jungen, J. Chem. Phys. 53, 4168 (1970).
[5] D. Zakheim and P. Johnson, J. Chem. Phys. 68, 3644 (1978).
[6] P. R. Blazewicz, X. Tang, R. N. Compton, and J.A.D. Stockdale, J. Opt. Soc. Am. 4, 770 (1987).
[7] J. C. Miller and R. N. Compton, J. Chem. Phys. 75, 22 (1981); 84, 675 (1985).
[8] G. Caprace, J. Delwiche, P. Natalis, and J. E. Collin, Chem. Phys. 13, 43 (1976).
[9] J. R. Appling, M. G. White, W. J. Kessler, R. Fernandez, and E. D. Poliakoff, J. Chem. Phys. 88, 2300 (1988).
[10] M. G. White, W. A. Chupka, M. Seaver, A. Woodward, and S. D. Colson, J. Chem. Phys. 80, 678 (1984).
[11] P. Lambropoulos, Phys. Rev. Lett. 28, 585 (1972); J. Phys. B 6, L319 (1973).
[12] S. Klarsfeld and A. Maquet, Phys. Rev. Lett. 29, 79 (1972).
[13] A. Lyras, B. Dai, X. Tang, P. Lambropoulos, A. Dodhy, J. A. D. Stockdale, D. Zei, and R. N. Compton, Phys. Rev. Lett. 37, 403 (1988).
[14] H. R. Reiss, Phys. Rev. Lett. 29, 1129 (1972).
[15] S. N. Dixit, J. Phys. B 14, L683 (1981).

J. Phys. B: At. Mol. Opt. Phys. 23 (1990) L15-L19. Printed in the UK

LETTER TO THE EDITOR

Angular distributions of electrons from the photodetachment of metastable He^-

J S Thompson†, D J Pegg†§, R N Compton‡‖ and G D Alton‡

† Department of Physics, University of Tennessee Knoxville, TN 37996, USA
‡ Oak Ridge National Laboratory, Oak Ridge, TN 37831, USA

Received 22 September 1989

Abstract. Energy- and angle-resolved photoelectron spectroscopy has been used to investigate the spectral dependences of the angular distributions of electrons photodetached from a beam of metastable He^- ions.

We report on the first measurements of the angular distributions of electrons ejected in the photodetachment of He^- ions formed in the metastable $(1s2s2p)^4P$ state. In the spectral range of the present experiment, $1.775 \leq h\nu \leq 2.456$ eV, photodetachment into either the $He(1s2s\ ^1S)+e^-$ or the $He(1s2p\ ^3P)+e^-$ continua is allowed. Thresholds for these processes lie at 0.0755 eV and 1.222 eV, respectively. These competing exit channels are resolved in the present electron spectroscopic measurements. Spin-dependent interactions for a light ion such as He^- are expected to have a negligible effect on the shape of the emission patterns. However, with the exception of H^-, the He^- ion represents the simplest system for probing the effects of correlation on electron emission following photodetachment.

The apparatus used in the present photoelectron spectroscopic measurements has been described in detail by Pegg *et al* (1987). It consists of a fast beam of He^- ions that is crossed perpendicularly by a beam of linearly polarised light from a pulsed dye laser. The tenuous He^- ion beam is produced by sequential double charge transfer when a momentum-analysed beam of He^+ ions is passed through a Li vapour cell. Alignment of the $He^-(^4P)$ state in its production by sequential double charge transfer is expected to be small at the ion beam energy (30 keV) used in the present experiment. In addition, the coupling, via the spin–orbit interaction, of any aligned orbital angular momentum vector to a randomly oriented spin vector over many precessional cycles should reduce an initial alignment to a negligible amount at the photon–negative-ion interaction region. Due to the unstable nature of the metastable He^- ion, there will be some depletion of the initial population of the ions of the beam via autodetachment. A differential depletion effect on the different fine-structure levels will result from their differential metastability. The population of the ions entering the photodetachment region will be dominated by the most weakly autodetaching $J=\frac{5}{2}$ component. The fine structure is far too small to be resolved in the measurements. The asymmetry parameters for all of the unresolved fine-structure lines are expected to be the same

§ Also with: Physics Division, Oak Ridge National Laboratory, Oak Ridge, TN 37831-6366, USA.
‖ Also with: Department of Chemistry, University of Tennessee, Knoxville, TN 37996, USA.

0953-4075/90/020015+05$03.50

in the *LS* coupling approximation (Cooper and Zare 1969), and so the non-statistical population of the levels arising from autodetachment should have no effect on the photoelectron angular distributions.

Photoelectrons, ejected from the interaction region in the direction of motion of the ion beam, are energy analysed by means of a spherical sector electron spectrometer. The angular distributions of the photoelectrons were measured by determining the yield of electrons as a function of the angle θ between the fixed collection direction and the variable direction defined by the plane of polarisation of the laser beam. For linearly polarised radiation and a randomly polarised target, the angular correlation between the incoming photon and the outgoing electron should take the form, $f(\theta) = 1 + \beta P_2(\cos\theta)$ in the electric dipole approximation. The quantity β is the asymmetry parameter which characterises the shape of the emission pattern and $P_2(\cos\theta)$ is the second-order Legendre polynomial. The apparatus was tested by measuring the spectral dependence of the angular distribution of electrons produced by photodetaching beams of D^- and Li^- ions. Since all the photon energies used were below the threshold for leaving the residual D and Li atoms in an excited state, the emission process should be well described by an independent electron model which neglects correlation. The observed $\cos^2\theta$ ($\beta = 2$) distribution at all photon energies is in agreement with the predictions of Cooper and Zare (1969). A kinematic correction to the angular distributions is made in all cases to account for the fact that the electrons are detached from fast-moving ions. In general, this transformation from the laboratory frame to the ion frame involves amplitude and phase factors that depend on the velocity of the ion beam. In forward-directed electron spectroscopy, however, the phase factor becomes zero.

Figure 1 shows the measured spectral dependence of β for the photodetachment channel $He^-(^4P) + h\nu \rightarrow He(^3S) + e^-$. In an independent electron description of the process, the p-orbital electron that is ejected is represented by continuum s and d waves. As a result of interferences between these partial waves, the value of β will,

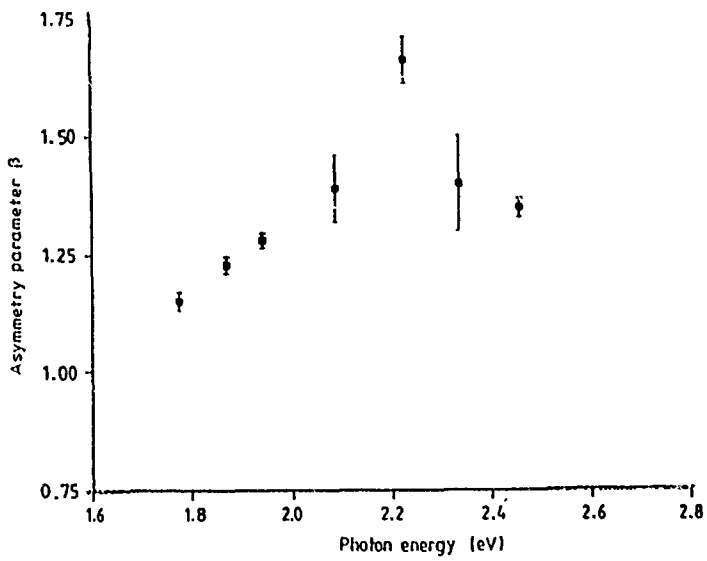

Figure 1. Spectral dependence of β for the photodetachment process $h\nu + He^-(^4P) \rightarrow He(^3S) + e^-$.

in general, change with photon energy. It might be expected, however, that the d waves would dominate the process so far above threshold. It is possible that the observed structure in β around 2.2 eV could be the result of the formation of a resonance by photoexcitation of an even parity state of the He^- ion. There are, however, no known resonances in this energy region. The most likely candidate would presumably be a quartet state associated with configurations such as 1s2s3s or 1s2s3d. Quartet resonances associated with the $n = 3$ states of the He atom have been studied by Oberoi and Nesbet (1973) but these calculations indicate that they all lie somewhat higher in energy than the region studied in the present work. It is also conceivable, though perhaps unlikely, that the observed structure in β shown in figure 1 is due to the presence of interchannel coupling via the final-state interaction, i.e. coupling between the common continuum final states associated with the $He(^3S)$ and $He(^3P)$ channels.

The observed spectral dependence of β for the channel $He^-(^4P) + h\nu \rightarrow He(^3P) + e^-$ is shown in figure 2. Here an s-orbital electron is ejected leading to a pure outgoing p-wave electron in the independent electron approximation. Neglecting correlation in the initial and final states, the angular distribution should take the form $\cos^2\theta$ ($\beta = 2$) for all photon energies. At the highest photon energy used in the experiment, the measured value of $\beta = 2$ is in agreement with the predictions of this model. As the photon energies are reduced toward threshold, however, the value of β is seen to decrease rather sharply over a small range of photon energies and then essentially level off at $\beta \approx 1.6$. Correlation effects in the initial state are expected to be small. Configuration-interaction calculations show that the lowest He^- state, $(1s2s2p)^4P$, is 96% pure (Bunge and Bunge 1979). In the case of photoionisation, it has been shown by Dill (1973) that anisotropic final-state interactions, which are neglected in the independent electron model, can have considerable effects on the photoelectron angular distributions. The outgoing electron can be reoriented, for example, by an exchange of angular momentum via electrostatic multipole forces. In the present case, the

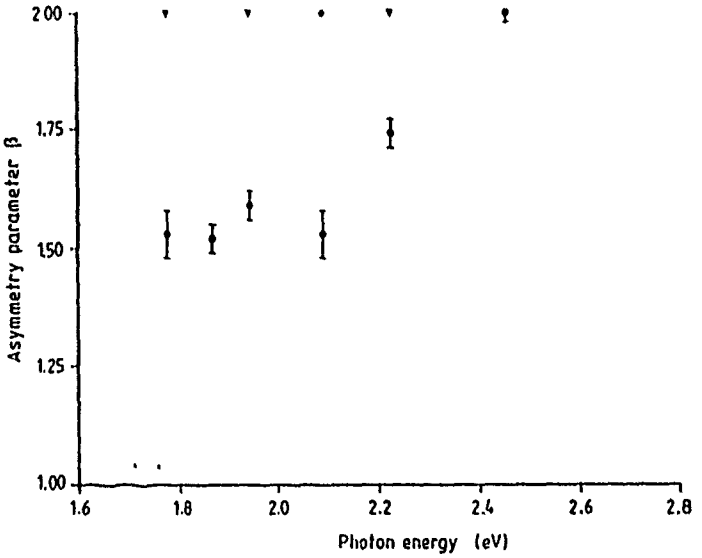

Figure 2. Spectral dependence of β for the photodetachment process $h\nu + He^-(^4P) \rightarrow He(^3P) + e^-$. The measurement technique was tested by photodetaching D^- (triangles) and Li^- (diamond).

residual He atom is left in the non-spherical, 2^3P excited state. The dominant electron–atom interaction will be the quadrupole force which, in principle, can exert a 'torque' on the outgoing electron. The permanent and induced dipole moments are expected to be small for this non-hydrogenic system.

The coupling of the continuum p-wave electron to the residual He(^{3}P) atom gives rise to $(1s2pkp)^4$S, ^{4}P and ^{4}D final states. In terms of the formalism of the angular momentum transfer theory of Fano and Dill (1972), this breakdown of the independent electron model results in angular momentum transfers of $j_t = 1$ and 2 in addition to $j_t = 0$. Each transfer is associated with a detachment scattering amplitude, $S_l(j_t)$. Here l refers to the orbital angular momentum of the outgoing electron. Manson and Starace (1982) show that the effective value of β under such conditions can be written as a weighted average of the form

$$\beta = \frac{\frac{2}{3}|S_1(0)|^2 - |S_1(1)|^2 + \frac{1}{3}|S_1(2)|^2}{\frac{1}{3}|S_1(0)|^2 + |S_1(1)|^2 + \frac{5}{3}|S_1(2)|^2}. \tag{1}$$

The relative moduli and phases of the scattering amplitudes will, in general, change as a function of the energy above threshold and this, in principle, could account for the decrease in β that is observed. In the case of photodetachment, however, the final-state interaction is expected to be short ranged and weak in comparison to the analogous situation in photoionisation. One might expect, therefore, that it would have a negligible effect on the photoelectron angular distributions.

An alternative explanation of the observed spectral dependence of β for the He(2^3P) exit channel involves a consideration of the influence of the $(1s2p^2)^4$P shape resonance on the emission process. This resonance has been experimentally studied by Peterson *et al* (1985) and theoretically investigated by Hazi and Reed (1981) and Watanabe (1982). It lies ~11 meV above the 2^3P threshold. The photon energies used in the present work correspond to a range of energies that lie ~0.5–1.0 eV, or approximately one hundred resonance widths, above the resonance. This very strong resonance has a calculated peak cross section of $\sim 8 \times 10^{-15}$ cm^2. The calculation of Watanabe (1982) indicates that even in the wings of this large resonance, ~0.8 eV above the peak, the resonance can make a non-negligible contribution to the photodetachment process. It seems plausible that the shape resonance could enhance the strength of the final-state interaction leading to the $(2s2skp)^4$P state as a result of the protracted time that the outgoing electron spends in the vicinity of the parent He atom. Recent theoretical results of Saha and Compton (1989) seems to confirm this resonant enhancement of the photodetachment process via the He(^{1}P) channel.

The presence of the shape resonance could have an effect on the angular distribution of photoelectrons. In the present experiment, the $(1s2p^2)^4$P resonant state of He$^-$ will be anisotropically excited. The photoexcitation process is necessarily state selective as a result of the use of linearly polarised incident radiation and the restriction imposed on the possible final states by the Pauli exclusion principle. The electrons subsequently ejected in the autodetachment of the resonance will carry away the anisotropy. It is estimated, in the independent electron approximation, that the emission pattern resulting from the autodetaching decay of this resonance is characterised by a value of $\beta = 0.5$, which is considerably smaller than the value of $\beta = 2$ expected from the non-resonant photodetachment process. The effect of the resonance on the emission process can be viewed in terms of an interference effect. The shape of the observed spectral dependence of β arises from an interference between non-resonant and resonant photodetachment pathways to the common $(1s2pkp)^4$P final state. The

measured value of β at a particular photon energy would then be the result of an appropriate weighting of the different β from the two pathways. It is expected that the weighting factors will be determined, as a function of the photon energy, by the relative cross sections for the two interfering processes. In the energy range of the present measurements, the non-resonant photodetachment process should dominate but the non-negligible contribution from the resonance process could be sufficient to perturb the angular distributions of the ejected photoelectrons.

In conclusion, an investigation has been made of the angular distribution of electrons ejected in the photodetachment of He^- via the two resolved exit channels that leave the He atom in either the 2^1S or the 2^3P state. It appears from the results that the independent electron model is inadequate to describe the emission process for either channel. Correlation, in some form, affects the photoelectron angular distributions. In the case of the $He(^3P)$ channel, the $(1s2p^2)^4P$ shape resonance may play a role in enhancing the photodetachment process and in perturbing the emission pattern. It is clear from this work that further theoretical working on the photodetachment of the relatively tractable, yet fundamentally interesting, He^- ion is needed to aid in a full quantitative understanding of the emission process.

We would like to acknowledge J Burgdörfer and A Starace for their helpful discussions. Two of us (JST and DJP) acknowledge research support from the US Department of Energy, Office of Basic Energy Sciences, Division of Chemical Sciences through the University of Tennessee. Two of us (RNC and GDA) acknowledge support from the US Office of Naval Research. Oak Ridge National Laboratory is operated by Martin Marietta Energy Systems, Inc under Contract No DE-AC05-840R21400.

References

Bunge A V and Bunge C F 1979 *Phys. Rev.* 19 452
Cooper J and Zare R N 1969 *Lectures in Theoretical Physics: Atomic Collision Processes* vol XI-C, ed S Geltman, K T Mahanthappa and W E Brittin (New York: Gordon and Breach) p 317
Dill D 1973 *Phys. Rev.* A 7 1976
Fano U and Dill D 1972 *Phys. Rev.* A 6 185
Hazi A U and Reed K 1981 *Phys. Rev.* 24 2269
Manson S T and Starace A F 1982 *Rev. Mod. Phys.* 54 389
Oberoi R S and Nesbet R K 1973 *Phys. Rev.* A 8 2969
Pegg D J, Thompson J S, Compton R N and Alton G D 1987 *Phys. Rev. Lett.* 59 2267
Peterson J R, Bae Y K and Huestis D L 1985 *Phys. Rev. Lett.* 55 692
Saha H and Compton R N 1989 Private communication to be published
Watanabe S 1982 *Phys. Rev.* 25 2074

Theoretical Studies of the Photophysics of $He^-(1s2s2p)\,^4P^o$

H. P. Saha
Department of Physics, University of Central Florida, Orlando, Florida 32816-0993

R. N. Compton
Oak Ridge National Laboratory, Oak Ridge, Tennessee 37831-6125

(Received 30 November 1989)

Cross sections and asymmetry (β_{nl}) parameters for the photodetachment of $2s$ and $2p$ electrons from $He^-(1s2s2p)\,^4P^o$ are calculated using the multiconfiguration Hartree-Fock method which includes the effects of dynamical core polarization and electron correlation. The excellent agreement with limited experimental data suggests its accuracy over the energy range from 0 to 4 eV. The photodetachment cross sections are used to calculate the inverse radiative attachment cross sections.

PACS numbers: 32.80.Fb

Negative-ion states which lie in the continuum and do not radiate to a lower state will eventually autodetach to a neutral plus a free electron. The lifetime of such autodetaching states depends upon the strength of the coupling to the continuum. Those states which interact strongly with the continuum via the electrostatic terms in the Hamiltonian are short-lived ($\sim 10^{-12}$–10^{-15} sec) and are observed as resonances in electron-scattering[1] or photodetachment[2] cross sections. Those states which interact weakly with the continuum via the spin-spin or spin-orbit interactions of the Hamiltonian can have autodetachment lifetimes approaching milliseconds. The $(1s2p2p)\,^4P^o$ state of He^- is a classic example of a long-lived Feshbach resonance (electron bound to an excited state). The $J=\frac{3}{2}$ and $\frac{1}{2}$ fine-structure components of $He^-\,^4P^o$ can decay[3] through spin-orbit and spin-spin interactions via coupling with the doublet P states, while the lower-level $^4P_{5/2}$ state can decay[4] only through the considerably weaker spin-spin interaction. Relativistic radiative autodetachment of $He^-\,^4P^o$ has not yet been detected. Many of the physical properties of metastable $He^-\,^4P^o$ have been extensively studied both experimentally and theoretically since its discoveries in 1925 and 1939 (Ref. 5) (for a brief review, see Ref. 6).

There have been a number of experimental measurements[7-11] and two theoretical calculations[12,13] concerning the photodetachment of $He^-\,^4P^o$. Both experiment[8-10] and theory[12] exhibit an enormous peak in the photodetachment cross section at ~ 1.2344 eV with a half-width of 7 meV. This peak is due to the excitation of the $He^-\,^4P^o$ state to the $(1s2p2p')\,^4P^e$ shape resonance. The experimentally determined maximum in the cross section is 80 ± 10 Å^2 and is about 3.3 times larger than the previous theoretical value[12] (~ 24 Å^2).

In this paper, the multiconfiguration Hartree-Fock (MCHF) method is used to calculate accurate photodetachment cross sections and angular distribution asymmetry parameters for $He^-\,^4P^o$ for incident photon energies from threshold to 4.5 eV. Comparison is made with existing cross-section measurements[7-11] and with recent asymmetry parameter measurements.[14] Finally, the principle of detailed balance is used to calculate the radiative attachment cross sections for $He(1s2s\,^3S)$.

Electron-correlation and dynamic core-polarization effects are very important in the accurate calculation of photodetachment properties of negative ions. Recently the MCHF method[15] was shown to reproduce[16] the previously calculated bound-free photodetachment cross section of H^- over the photon energy range from 0.8 to 3 eV. As in the present calculations, the electron-correlation and dynamic core-polarization effects were accounted for in an *ab initio* manner. The accuracy of the MCHF method exhibited for H^- suggested its application to the more complicated case of $He^-(1s2s2p\,^4P^o)$. The excellent agreement between the length and velocity calculations for both H^- and the present He^- case attest to the accuracy and completeness of the initial- and final-state wave functions. Details of the present calculations along with partial cross sections will appear in a separate publication by Saha.

The initial and final states considered in the present calculation are

$$\begin{aligned} h\omega + He^-(1s2s2p\,^4P^o) &\rightarrow He(^3S)+e(ks)\,^4S^e \\ &\rightarrow He(^3S)+e(kd)\,^4D^e \\ &\rightarrow He(^3P)+e(kp)\,^4S^e \\ &\rightarrow He(^3P)+e(kp)\,^4P^e \\ &\rightarrow He(^3P)+e(kp)\,^4D^e. \end{aligned} \quad (1)$$

We emphasize that relativistic effects are not included, and therefore any fine-structure effects (J dependence) on the initial ion or final state are not included. Future studies would include calculations of σ and β for the individual $J=\frac{5}{2}$, $\frac{3}{2}$, and $\frac{1}{2}$ levels of $He^-\,^4P^o$.

The MCHF expansion of the wave function for the in-

itial state consisted of configurations constructed from $1s$, $2s$, $2p$, $3s$, $3p$, $3d$, $4s$, $4p$, $4d$, $4f$, $5s$, $5p$, $5d$, $6s$, $6p$, and $6d$ orbitals. All of the bound orbitals are optimized variationally.[17] The five final-state wave functions were made from expansions of the configurations coupled to form each of the $^4S^e$, $^4P^e$, and $^4D^e$ terms. The electron affinity for He(2^3S) was calculated to be 0.0775 eV and is in exact agreement with the more accurate value of 0.077 51 ± 0.000 04 eV of Bunge and Bunge.[18] The electron affinity for He(2^3P) was 1.221 eV which is in excellent agreement with the experimental value of 1.222 ± 0.0008 eV.[9]

The photodetachment cross section for absorbing a photon of energy $\hbar\omega$ from an initial state i to a final state f is given by

$$\sigma(\omega) = 4\pi^2 \alpha a_0^2 \omega \sum_{f,m} |\langle \psi_f | T | \psi_i \rangle|^2 , \tag{2}$$

where α is the fine-structure constant and a_0 is the radius of the first Bohr orbit of the H atom. ψ_i and ψ_f represent the wave functions describing the bound and free states of the negative ion. The summation runs over all of the final configurations and magnetic quantum numbers. The length and velocity forms of the dipole transition operator T are

$$T_L = \sum_{j=1}^{n} z_j \text{ and } T_V = \sum_{j=1}^{n} \frac{\nabla_j}{i\omega} . \tag{3}$$

ψ_i and ψ_f are found to be exact solutions of the same Hamiltonian if the length and velocity forms of the cross sections and β parameters are identical. The method of constructing the MCHF wave function for the final continuum state involves the solution of coupled integro-differential equations which are solved by an iterative method and is identical to that described in detail earlier.[16]

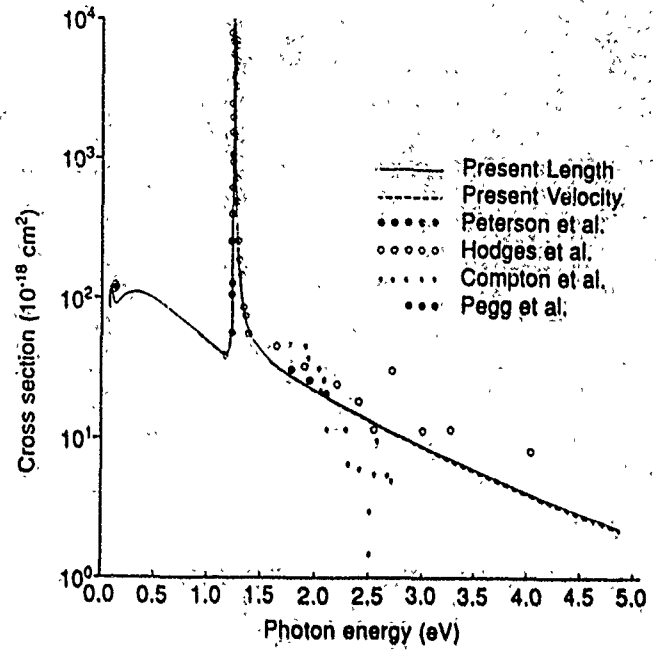

FIG. 1. Total photodetachment cross sections for $He^-(^4P^o)$ vs photon energy.

The angular distribution of photoelectrons detached from a subshell, nl, by light polarized in the $\hat{e}$ direction is related to the differential cross section by the relation

$$\frac{d\sigma_{nl}(\omega)}{d\Omega} = \frac{\sigma_{nl}(\omega)}{4\pi}[1 + \beta_{nl}(\omega) P_2(\hat{e}\cdot\hat{k})] . \tag{4}$$

P_2 is the second-order Legendre polynomial whose argument is the cosine of the angle between the polarization vector $\hat{e}$ and the direction of the outgoing electron $\hat{k}$. The asymmetry parameter $\beta_{nl}(\omega)$ for the photodetachment of the $2p$ electron from $He^-\ ^4P^o$ was calculated using the Cooper-Zare model,[19]

$$\beta_{nl}(\omega) = \frac{l(l-1)T_{l-1}^2(\omega) + (l+1)(l+2)T_{l+1}^2(\omega) - 6l(l+1)T_{l-1}(\omega)T_{l+1}(\omega)\cos(\xi_{l+1} - \xi_{l-1})}{(2l+1)[lT_{l-1}^2(\omega) + (l+1)T_{l+1}^2(\omega)]} , \tag{5}$$

where $T_{l-1}(\omega)$ and $T_{l+1}(\omega)$ are the radial parts of the dipole matrix element corresponding to the $l-1$ and $l+1$ channel, respectively, and ξ_l is the phase shift of the lth channel. The use of the Cooper-Zare model for an s subshell[20] gives a value of 2 for β since differences of the photoelectron phase shifts for the last three channels in Eq. (4) are ignored. These phase-shift differences are taken into account in the angular momentum transfer formalism.[21] Following the formalism of Fano and Dill,[22] β for an s subshell is given by

$$\beta = \frac{\sum_{j_t} \sigma(j_t)\beta(j_t)}{\sum_{j_t} \sigma(j_t)} . \tag{6}$$

In the LS-coupling approximation[20]

$$\hat{j}_t = \hat{L}_c - \hat{L}_0 ,$$

where $\hat{L}_0$ and $\hat{L}_c$ are the orbital angular momentum of the initial and final core states, respectively.

Figure 1 shows the total cross section obtained by summing up the partial photodetachment cross sections. The experimental value of Compton, Alton, and Pegg,[7] Peterson and co-workers,[9,10] and Pegg *et al.*[11] are shown for comparisons. The total cross section rises sharply from the He(2^3S) threshold to a maximum of 1.2 Å^2 at 0.085 eV then decreases to a minimum at about 0.125 eV. This rapid rise and fall of the cross section is due to the $1s2s(^3S)ks\ ^4S^e$ channel. The broad maximum in the cross section around 0.3 eV is due to the $1s2s(^3S)kd\ ^4D^e$ channel. At higher photon energy the photodetachment cross section is dominated by the $1s2p^2\ ^4P^e$ shape resonance. The resonance position and

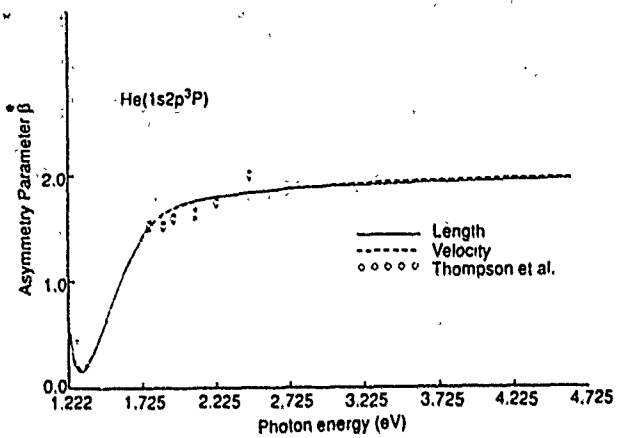

FIG. 2. Photoelectron asymmetry parameters, β_{2s}, as a function of photon energy.

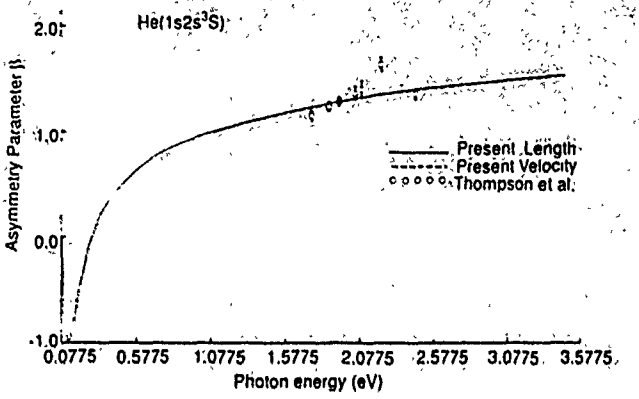

FIG. 3. Photoelectron asymmetry parameters, β_{2p}, as a function of photon energy.

width (FWHM) are calculated to be 1.231 and 0.0075 eV which are in excellent agreement with the experimental value of 1.2344 ± 0.0004 and 0.0070 ± 0.0004 eV, respectively.[10] It is seen from the figure that there is outstanding agreement between the present results and the absolute cross sections of Peterson, Bae, and Huestis[10] in the vicinity of the resonance. Early data of Peterson, Coggiola, and Bae[9] also indicated that additional structure might be present below 1.23 eV suggestive of possible interference from ^4S or ^4D states in this energy region; however, their later measurements showed no structure.[10] The present calculations also show no such interference structure. Compton, Alton, and Pegg[7] also report structure at 2.5 eV which was not present in our calculations. In fact, no evidence for any other resonance structure was found up to ~5 eV. Finally, we note almost exact agreement with the cross sections determined by Pegg *et al.*[11] which are expected to be the most accurate experimental measurements to date.

The asymmetry parameters $\beta_{nl}(\omega)$ for the photodetachment of $2s$ and $2p$ electrons are presented in Figs. 2 and 3, respectively, along with the limited experimental data recently available.[14] Again the near equivalence of the length and velocity results attest to the accuracy of the wave functions representing the initial and final states. Figure 2 shows the calculated $\beta_{2s}(\omega)$ for photodetachment of the $2s$ electron. Agreement between experiment and theory is very good over the energy range available from experiment. The distribution is nearly isotropic at threshold and approaches asymptotically the Cooper-Zare model value of 2 [Eq. (5)]. The asymmetry parameters for the $2p$ electron, $\beta_{2p}(\omega)$, in Fig. 3 varies from 0 to -1 in a narrow region above threshold and approaches 1.5 asymptotically. Thus, the angular distribution of photoelectrons would be isotropic at threshold and quickly changing to $\sin^2\theta$ dependence (ejected perpendicularly to the plane of polarization of the photon beam). The experimental data and theory are seen to agree very well for $\beta_{2p}(\omega)$ over the narrow energy region.

The principle of detailed balance can be used to relate the photodetachment cross section σ_d to the radiative attachment cross section, σ_a,

$$\sigma_a = \left(\frac{h\nu}{mvc}\right)^2 \frac{g^-}{g^0}\sigma_d, \tag{7}$$

where ν is the frequency of the quantum emitted, m is the mass of the electron, v its velocity, and g^-/g^0 is the ratio of the statistical weights of the negative ion and atomic states (taken to be 4 here).[23] The radiative attachment cross sections to metastable $He(1s2s)^3S$ are shown in Fig. 4 as a function of electron energy ranging from 0.00136 to 2.5 eV. Experimental cross sections of Pegg *et al.*[11] are included. Also shown are cross sections at two energies from Hodges, Coggiola, and Peterson.[8]

This research was supported by the National Science Foundation under Grant No. PHY-8801881, in part by a Cottrell Research Grant from the Research Corporation, and by the U.S. Office of Naval Research, Grant No. ONR N00014-89-J-1787. Acknowledgment is also made to the donors of the Petroleum Research Fund administered by the American Chemical Society for partial

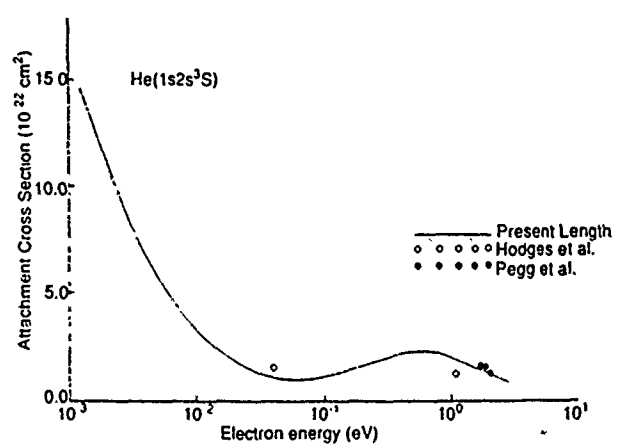

FIG. 4. Radiative attachment cross sections vs electron energy.

support of this research and the Florida State University through time granted on its Cyber 205 Supercomputer. This research was sponsored by the Office of Health and Environmental Research and the U.S. Department of Energy under Contract No. DE-AC05-84OR21400 with Martin Marietta Energy Systems, Inc.

[1]G. J. Schulz, Rev. Mod. Phys. **45**, 378 (1973).

[2]T. A. Patterson, H. Hotop, A. Kasdan, D. W. Norcross, and W. C. Lineberger, Phys. Rev. Lett. **32**, 189 (1974).

[3]C. A. Nicolaides, Y. Kominos, and D. R. Beck, Phys. Rev. **24**, 1103 (1981), and references therein.

[4]J. L. Pietenpol, Phys. Rev. Lett. **7**, 64 (1961).

[5]von Julius W. Hiby, Ann. Phys. (Paris) **34**, 473 (1939); although Hiby has generally received credit for the first He^- observation, one report of He^- goes back to 1925 [R. Döpel, Ann. Phys. (Leipzig) **76**, 1 (1925)]. This paper also reports weak signals of H_2^- ions which likely represents the first observation of the deuteron. H_2^- is not believed to be stable.

[6]G. D. Alton, R. N. Compton, and D. J. Pegg, Phys. Rev. **28**, 1405 (1983).

[7]R. N. Compton, G. D. Alton, and D. J. Pegg, J. Phys. B **13**, L651 (1980).

[8]R. V. Hodges, M. J. Coggiola, and J. R. Peterson, Phys. Rev. A **23**, 59 (1981).

[9]J. R. Peterson, M. J. Coggiola, and Y. K. Bae, Phys. Rev. Lett. **50**, 664 (1983).

[10]J. R. Peterson, Y. K. Bae, and D. L. Huestis, Phys. Rev. Lett. **55**, 692 (1985).

[11]D. J. Pegg, J. S. Thompson, J. Dellwo, R. N. Compton, and G. D. Alton, Phys. Rev. Lett. **64**, 278 (1990).

[12]A. U. Hazi and K. Reed, Phys. Rev. A **24**, 2269 (1981).

[13]L. V. Chernysheva, G. F. Gribakin, V. K. Ivanov, and M. Vu. Kuchiev, J. Phys. B **21**, L419 (1988).

[14]J. S. Thompson, D. J. Pegg, R. N. Compton, and G. D. Alton, J. Phys. B **23**, L15 (1990).

[15]H. P. Saha, M. S. Pindzola, and R. N. Compton, Phys. Rev. A **38**, 128 (1988).

[16]H. P. Saha, Phys. Rev. A **38**, 4546 (1988).

[17]C. F. Fischer, Comput. Phys. Commun. **14**, 145 (1978).

[18]A. V. Bunge and C. F. Bunge, Phys. Rev. A **30**, 2179 (1984).

[19]J. Cooper and R. N. Zare, in *Lectures in Theoretical Physics*, edited by S. Geltman, K. Mahanthappa, and W. Britten (Gordon and Breach, New York, 1969), Vol. 11e, pp. 317–337.

[20]S. T. Manson and A. F. Starace, Rev. Mod. Phys. **54**, 389 (1982).

[21]D. Dill, S. T. Manson, and A. F. Starace, Phys. Rev. Lett. **32**, 971 (1974).

[22]U. Fano and D. Dill, Phys. Rev. A **6**, 185 (1972); D. Dill, and U. Fano, Phys. Rev. Lett. **29**, 1023 (1972).

[23]g^-/g^0 is equal to the ratio of $(2S+1)(2L+1)$ for $He^-(^4P^o)$ to $He(^3S)$ or $(4\times3)/(3\times1)=4$.

Partial Cross Sections for the Photodetachment of Metastable He^-

D. J. Pegg,[a] J. S. Thompson,[b] and J. Dellwo
Department of Physics, University of Tennessee, Knoxville, Tennessee 37996

R. N. Compton[c] and G. D. Alton
Oak Ridge National Laboratory, Oak Ridge, Tennessee 37831
(Received 3 October 1989)

Partial cross sections for the photodetachment of a $2s$ or $2p$ electron from metastable $(1s2s2p)^4P$ He^- ions have been determined using crossed-beam photoelectron spectroscopy. Kinematic effects associated with detachment from a fast beam source have been exploited, in a novel way, to enhance the precision of the measurements. Calculated cross sections for the photodetachment of H^- were used to establish a scale for the He^- measurements. Radiative attachment cross sections are derived from the photodetachment results using the principle of detailed balance.

PACS numbers: 32.80.Fb

The three-electron He^- ion has a relatively simple structure. As such, it has received a great deal of experimental and theoretical attention since its discovery by Hiby.[1] It is well known that stable He^- ions are nonexistent due to the fact that an electron is unable to attach itself to a He atom in its ground state. The He^- ion is instead the prototype of an unusual class of unstable, yet long-lived, negative ions that are metastable against decay via electron (autodetachment) and photon (electric dipole) emission. The ion is formed in the core-excited and spin-aligned $(1s2s2p)^4P$ state when an electron attaches itself to a He atom in the metastable $(1s2s)^3S$ excited state. Autodetachment via the strong electrostatic interactions is spin forbidden. The process proceeds, however, at a slower rate via the weaker magnetic interactions among the electrons. There exist a differential metastability among the fine-structure levels due to their different coupling strengths to the continuum. The lifetimes of the three levels and their relative spacings have been measured by Novick and co-workers.[2] The He^- ion lives long enough (tens to hundreds of microseconds) that a beam of ions can be formed in an accelerator and subsequently used as an essentially stable source for experiments. The structure of He^- is now well established. The electron affinity of $He(2^3S)$ has been calculated by Bunge and Bunge[3] to be 77.51 ± 0.04 meV. This quantity was first measured by Brehm, Gusinow, and Hall[4] using crossed laser-ion-beam photoelectron spectroscopy and later by Peterson, Bae, and Huestis[5] using a merged-beam threshold photodetachment technique. The latter value is in excellent agreement with theory.

The detailed manner in which metastable ions such as the He^- ion interact with radiation is not as well known, however, although the subject is of fundamental interest. In particular, experimental data on absolute partial cross sections, which are the subject of this paper, are sparse. The simplest stable negative ion, H^-, has a single open photodetachment channel, $h\nu + H^-(1^1S) \rightarrow H(1^2S) + e^-(kp)$, in the visible ($h\nu < 10.96$ eV). In contrast, photodetachment of He^- can lead to five possible final (continuum) states in the visible ($h\nu < 4.85$ eV); i.e., ^4S and ^4D states associated with the process $h\nu + He^-(2^4P) \rightarrow He(2^3S) + e^-(ks,d)$ and ^4S, ^4P, and ^4D states associated with the process $h\nu + He^-(2^4P) \rightarrow He(2^3P) + e^-(kp)$. The technique of energy and angle-resolved photoelectron spectroscopy has allowed us to quantitatively investigate, as a function of photon energy, the competition between the two resolved photodetachment processes that leave the He atom in the 2^3S and 2^3P states, respectively. The partial cross sections, $\sigma(^3S)$ and $\sigma(^3P)$, for the two processes have each been measured relative to the known cross section, $\sigma(^2S)$, for photodetaching a reference D^- ion. As far as it is known, the present data represent the only published measurement of branching ratios for competing photodetachment channels. At the present time there are no published calculations of the partial cross sections for He^- photodetachment, although work is currently in progress.[6]

The cross-section ratios were determined from measurements of the yields and angular distributions of photoelectrons ejected from the ions at the intersection of crossed laser- and negative-ion beams. The fast moving ($\sim$30 keV) and tenuous beam of negative ions was produced by double charge exchange between a beam of positive ions and atoms in a Li vapor cell. The negative-ion beam was intersected orthogonally by a linearly polarized beam of photons from a flashlamp-pumped pulsed dye laser. Sets of apertures were used to ensure that the overlap of the two beams remained unaltered during the relative measurement process. Following photodetachment events, electrons ejected from the He^- ions, in the direction of motion of the ion beam (forward-directed electrons), were collected and energy analyzed using a spherical-sector electron spectrometer.

The angular distributions of the detached electrons were determined by measuring their yields as a function of the angle between the fixed collection direction and the direction defined by the polarization vector of the laser beam. The polarization vector could be rotated in a plane perpendicular to the propagation direction of the laser by the use of a $\lambda/2$ phase retarder (double Fresnel rhomb). The output power of the laser was carefully chosen to avoid saturation on each of the photodetachment processes studied. The instantaneous intensities of the photon and ion beams were monitored for normalization purposes. A synchronous detection scheme, based on the time structure of the pulsed laser, was used to discriminate against the rather large electron background. Further details of this crossed-beams apparatus can be found in a previous publication.[7]

The relative cross sections (angular integral) were obtained by comparing, under identical geometrical conditions, the yields of electrons, Y(He) and Y(D), produced in the photodetachment of beams of He^- and D^- ions, respectively. The cross-section ratio for these two processes can be expressed by the following relation:

$$\frac{\sigma(\mathrm{He})}{\sigma(\mathrm{D})} = \frac{Y(\mathrm{He})\phi(\mathrm{D})\rho(\mathrm{D})g(\mathrm{D})[1+\beta(\mathrm{D})]}{y(\mathrm{D})\phi(\mathrm{He})\rho(\mathrm{He})g(\mathrm{He})[1+\beta(\mathrm{He})]} . \quad (1)$$

In this expression the yield ratio is multiplied by several measured factors that take account of the different photon fluxes, ϕ, ion densities, ρ, frame-transformed solid-angle factors, g, and asymmetry parameters, β, associated with photodetaching electrons from the two beams. All geometric factors are adjusted to be equal and therefore cancel out. A novel technique, which is illustrated in Fig. 1, has been used to cancel out the efficiency factors associated with the collection and detection of electrons from the two beams. The three photoelectron spectral peaks shown in Fig. 1, which have different energies in the ion frame, can be kinematically shifted to the same energy in the laboratory frame by an appropriate choice of the ion-beam energies, E_i. The efficiencies for collecting and detecting electrons of the same energy from the He^- and D^- beams then become equal and cancel out. The ion-beam energies, which are needed to determine both the ion densities and solid-angle transformation factors shown in Eq. (1), can be determined precisely (—0.1%) from an *in situ* analysis of the separation of the peaks in the photoelectron spectra. For example, the He^- photodetachment spectrum consists of a pair of peaks (one for each exit channel) whose separation in the ion frame, $E(^3S\text{-}^3P)$, is well known from photon spectroscopy. A determination of their separation in the laboratory frame can then be used to measure the ion-beam energy. This technique, which depends on either kinematic shifting or doubling of the spectral lines, is described in more detail by Pegg *et al.*[7] Angle-resolved yield measurements were made on each spectral line to determine the asymmetry parameters β that characterize the shape of the photoelectron emission patterns. The measurement technique was first tested by photodetaching electrons from beams of D^- and Li^- ions. The predicted $\cos^2\Theta$ ($\beta=2$) distribution was obtained in all cases. The ^3P exit channel in He^- photodetachment involves the ejection of an s orbital electron, similar to

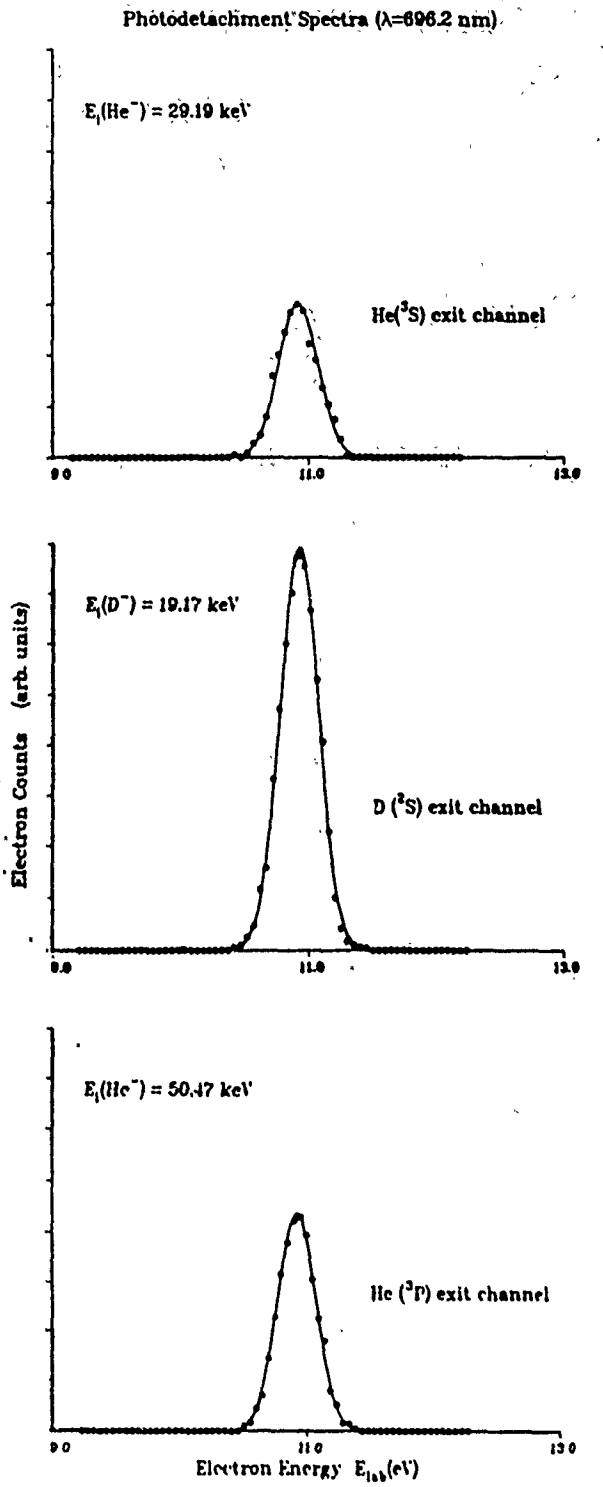

FIG. 1. Three spectral peaks kinematically shifted to the same laboratory-frame energy by an appropriate choice of ion-beam energies. The peak yields were used in the measurement of relative cross sections for the photodetachment of He^- and D^- ions.

photodetachment in the stable D^- and Li^- ions. The measured values of β, however, are considerably smaller ($\beta \sim 1.5$) than the $\beta = 2$ predicted by an independent-electron model. It is suspected that the presence of the $(1s2p^2)^4P$ shape resonance[5] lying just above the threshold for the opening of the ^3P channel is perturbing the angular distribution of the photoelectrons in this case. The spectral dependence of the asymmetry parameters characterizing the angular distribution of electrons ejected in the photodetachment of He^- are the subject of a paper by Thompson *et al.*[8] Calculations have been made by Saha and Compton.[6]

The partial cross-section ratios, $\sigma(^3S)/\sigma(^2S)$ and $\sigma(^3P)/\sigma(^2S)$, have been measured at photon energies of 1.781, 1.946, and 2.091 eV. The results are $\sigma(^3S)/\sigma(^2S) = 0.60 \pm 0.02$ (1.781 eV), 0.57 ± 0.04 (1.946 eV), and 0.49 ± 0.04 (2.091 eV); $\sigma(^3P)/\sigma(^2S) = 0.28 \pm 0.02$ (1.781 eV), 0.18 ± 0.02 (1.946 eV), and 0.12 ± 0.01 (2.091 eV). The uncertainties quoted on these values represent 2 standard deviations of the weighted mean of several data sets each comprising a number of individual spectra added together. The major source of statistical error in each data set originates in the measurement of yield ratios (~4%) and asymmetry-parameter ratios (~3%). Uncertainties in other measured quantities are considered to be negligible. Systematic error sources have been investigated and are estimated to be within the quoted 2σ limits. A scale for the relative cross-section measurements can be readily established by assuming theoretical values for the $\sigma(^2S)$ cross section for photodetaching the D^- ion. Several calculations of H^- photodetachment cross sections have been made and can be used for this purpose. The perturbation-variation results of Stewart[9] have been arbitrarily chosen for the purpose of normalization in the present work. The results of Broad and Reinhardt[10] fall within 2% of those of Stewart over the range of the present experiments. Combining the theoretical values (assuming a 3% uncertainty) with the measured cross-section ratios produces the partial cross sections (in Mb) shown in Table I. The sum of the partial cross sections, σ_{total}, and the measured asymmetry parameters, β, are also tabulated. The branching ratios for the ^3S channel are 0.70 ± 0.06 (1.781 eV), 0.75 ± 0.10 (1.946 eV), and 0.80 ± 0.18 (2.091 eV). The measured partial and total cross sections are also shown in Fig. 2, along with the results of the total cross-section calculation of Hazi and Reed.[11] The calculation and the sum of the present partial cross-section measurements are seen to be in good agreement at all the photon energies used in the experiment. The only other partial cross-section measurement for He^- is that of Brehm, Gusinow, and Hall.[4] Their estimates, at a photon energy of 2.410 eV, are limited in precision to a factor of 2 since no angular distribution information was obtained in the experiment. The less precise total cross-section measurements of Compton, Alton, and Pegg[12] and Hodges, Coggiola, and Peterson[13] are in essential agreement with the sum of the partial cross sections measured here.

TABLE I. Photodetachment of He^-: cross sections (Mb) and asymmetry parameters.

	Photon energy (eV)		
	1.781	1.946	2.091
$\sigma(^3S)$	22.9 ± 1.0	20.5 ± 1.5	16.6 ± 1.8
$\beta(^3S)$	1.15 ± 0.02	1.28 ± 0.02	1.19 ± 0.07
$\sigma(^3P)$	10.0 ± 0.6	6.7 ± 0.6	4.1 ± 0.4
$\beta(^3P)$	1.52 ± 0.04	1.59 ± 0.03	1.53 ± 0.05
σ_{total}	32.9 ± 2.4	27.2 ± 3.1	20.7 ± 3.0

The measured cross sections for photodetaching an electron from the He^- ion can be used to indirectly determine, using detailed balance arguments,[14] the cross sections, σ_a, for the far less probable inverse process of radiative attachment. The derived radiative attachment cross sections (in barns) are $\sigma_a(^3S) = 166 \pm 7$ (1.781 eV), 162 ± 12 (1.946 eV), and 120 ± 13 (2.091 eV); $\sigma(^3P) = 74 \pm 5$ (1.781 eV), 45 ± 4 (1.946 eV), and 30 ± 3 (2.091 eV).

The relatively high precision (~5% in favorable cases) of the present cross-section ratio measurements reflects our ability to exploit, in a novel way, certain kinematic effects associated with a fast moving source of ions and the simultaneous collection of electrons in the forward direction. These features of the present apparatus have not been used in previous photodetachment

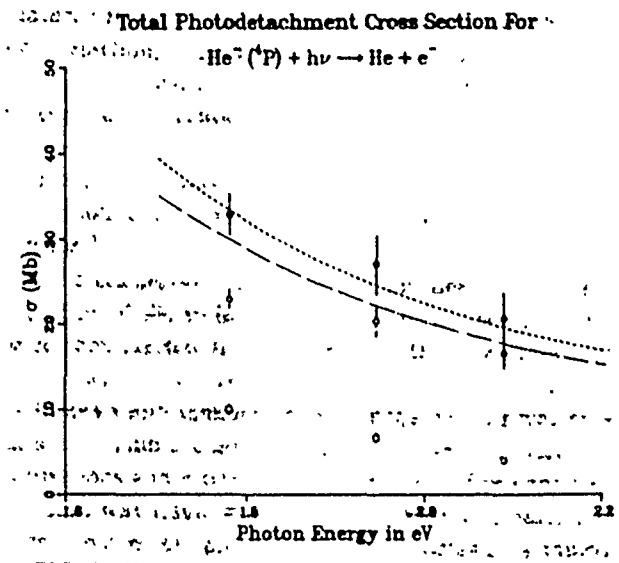

FIG. 2. The open squares and circles represent the partial cross sections for photodetaching He^- via the $He(^3P)$ and $He(^3S)$ exit channels, respectively. The solid circles, which are the sum of the partial cross sections, are compared with the results of the total cross-section calculation of Ref. 11 (shown as continuous curves). The length and velocity forms are represented by the upper and lower curves, respectively.

studies. A scale for the relative measurements has been established by the use of accurate theoretical values for the cross sections for the photodetachment of the reference ion, D^-. As a result we have been able to determine partial cross sections for the photodetachment of He^- to $< 10\%$.

This research was supported by the U.S. Department of Energy, Office of Basic Energy Sciences, Division of Chemical Sciences through the University of Tennessee. Oak Ridge National Laboratory is operated by Martin Marietta Energy Systems, Inc., under Contract No. DE-AC05-84OR21400 with the U.S. Department of Energy.

---

[a]Also at Physics Division, Oak Ridge National Laboratory, Oak Ridge, TN 37831.

[b]Present address: Joint Institute for Laboratory Astrophysics, Boulder, CO 80309.

[c]Also at Department of Chemistry, University of Tennessee, Knoxville, TN 37996.

[1]J. W. Hiby, Ann. Phys. (Leipzig) **34**, 473 (1939).

[2]R. Novick and D. Weinflash, in *Proceedings of the International Conference and Fundamental Constants, Gaithersburg, Maryland*, edited by D. N. Langenberg and B. N. Taylor (National Bureau of Standards Special Publication No. 343), pp. 403–410; D. L. Mader and R. Novick, Phys. Rev. Lett. **32**, 185 (1974).

[3]A. V. Bunge and C. F. Bunge, Phys. Rev. A **19**, 452 (1979).

[4]B. Brehm, M. A. Gusinow, and J. L. Hall, Phys. Rev. Lett. **19**, 737 (1967).

[5]J. R. Peterson, Y. K. Bae, and D. L. Huestis, Phys. Rev. Lett. **55**, 692 (1985).

[6]H. Saha and R. N. Compton (private communication); (to be published).

[7]D. J. Pegg, J. S. Thompson, R. N. Compton, and G. D. Alton, Nucl. Instrum. Methods Phys. Res., Sect. B **40/41**, 221 (1989).

[8]J. S. Thompson, D. J. Pegg, R. N. Compton, and G. D. Alton, J. Phys. B (to be published).

[9]A. L. Stewart, J. Phys. B **11**, 3851 (1978).

[10]J. T. Broad and W. P. Reinhardt, Phys. Rev. A **14**, 2159 (1976).

[11]A. U. Hazi and K. Reed, Phys. Rev. A **24**, 2269 (1981).

[12]R. N. Compton, G. D. Alton, and D. J. Pegg, J. Phys. B **13**, L651 (1980).

[13]R. V. Hodges, M. J. Coggiola, and J. R. Peterson, Phys. Rev. A **23**, 59 (1981).

[14]*Atomic Collisions: Electron and Photon Projectiles*, edited by E. W. McDaniel (Wiley, New York, 1989), p. 530.

Photoelectron Angular Distributions for ns ($n=8-12$) Subshells of Cesium: Relativistic Effects

L. E. Cuéllar
Department of Physics, The University of Tennessee, Knoxville, Tennessee 37996

R. N. Compton[a] and H. S. Carman, Jr.
Oak Ridge National Laboratory, Oak Ridge, Tennessee 37831

C. S. Feigerle
Department of Chemistry, The University of Tennessee, Knoxville, Tennessee 37996
(Received 8 March 1990)

Photoelectron angular distributions for resonantly enhanced three-photon ionization (2+1) of cesium via the ns ($n=8-12$) states have been measured. The asymmetry parameter β is found to vary from +1.2 for the 8s state to −0.5 for the 12s state. These results provide the first clear experimental evidence for relativistic (spin-orbit) effects on the photoelectron angular distribution for an alkali-metal atom.

PACS numbers: 32.80.Rm

The photoionization of an atom represents one of the most elementary collision processes. Photoionization of a randomly oriented ensemble of atoms is characterized by the total cross section σ and the asymmetry parameter β, which describes the angular distribution of photoelectrons. At low photon energies (wavelength of light much larger than the size of the atomic target) the electric dipole approximation is valid, and the differential cross section for photoionization by linearly polarized light is given by[1,2]

$$\frac{d\sigma(\epsilon)}{d\Omega}=\frac{\sigma(\epsilon)}{4\pi}[1+\beta(\epsilon)P_2(\cos\theta)], \tag{1}$$

where θ is the direction of the photoelectron with respect to the electric-field vector of the incident light, and $P_2(\cos\theta)$ is the second-order Legendre polynomial. σ and β are dependent upon the photoelectron energy ϵ and the bound and continuum wave functions involved. For LS coupling of nonrelativistic single-particle wave functions, β is given by[2]

$$\beta(\epsilon)=\frac{l(l-1)R_{l-1}^2+(l+1)(l+2)R_{l+1}^2-6l(l+1)R_{l-1}R_{l+1}\cos\delta}{(2l+1)[lR_{l-1}^2+(l+1)R_{l+1}^2]}, \tag{2}$$

where R_{l-1} and R_{l+1} are the radial matrix elements between the bound and continuum wave functions for the $l-1$ and $l+1$ partial waves, respectively. $\delta=\delta_{l+1}-\delta_{l-1}$ is the difference in the phase shifts for the two possible continuum functions. The important point in the present context is that, for photoionization from a pure s orbital ($l=0$) and when the phase-shift difference is zero, Eq. (2) predicts that β is independent of energy and is identically equal to 2. It has been shown, however, that deviations from this expectation may result when (a) anisotropic electron-ion interactions are important (e.g., photoionization from open-shell systems)[3-6] or (b) relativistic (spin-orbit) interactions are appreciable.[7-12] Anisotropic electron-ion interactions are absent for photoionization of the s states of alkali-metal atoms (closed-shell core) and deviations from $\beta=2$ thus provide a direct test of relativistic interactions. In this Letter we report photoelectron angular distributions for resonantly enhanced three-photon ionization (2+1) of cesium atoms via the 8s, 9s, 10s, and 12s states. In general, multiphoton excitation can give rise to aligned (spatially anisotropic) target states for which the form of the differential cross section is more complicated than that given in Eq. (1). In the present case, excitation of an ns state ($J=\frac{1}{2}$) results in an isotropic target, and Eq. (1) is valid. Values of β are found to vary from +1.2 for the 8s state to −0.5 for the 12s state which we attribute to relativistic (spin-orbit) effects in the photoionization continuum.

The importance of spin-orbit interactions in the heavy alkali-metal atoms has been recognized for many years. In 1930, Fermi[13] showed that spin-orbit interactions are responsible for the anomalous doublet-line-strength ratios for cesium. Seaton[14] later showed that inclusion of spin-orbit effects can result in nonzero minima in the photoionization cross sections (the so-called Cooper minima[15]). Fano[16] predicted that spin-orbit effects would result in emission of spin-polarized electrons when circularly polarized light is used to ionize Cs atoms. Experimental observations of the Fano effect soon followed,[17-19] and it was shown that accurate values for the position of the Cooper minimum could be obtained from the spin-polarization measurements.[19] Several theoretical studies have addressed the effects of spin-orbit interactions on photoelectron angular distributions,[7-12] but

experimental studies have been sparse.

Inclusion of relativistic (spin-orbit) effects results in radial matrix elements which depend upon the total angular momentum (j') of the continuum wave function. β for an s state then becomes[8,9,12]

$$\beta(\epsilon) = \frac{2R_{3/2}^2 + 4R_{1/2}R_{3/2}\cos(\delta_{3/2} - \delta_{1/2})}{2R_{3/2}^2 + R_{1/2}^2}. \quad (3)$$

It has been shown[8-11,16] that the phase-shift difference $\delta_{3/2} - \delta_{1/2}$ is generally close to zero. Under this condition note that when the matrix elements $R_{1/2}$ and $R_{3/2}$ are equal, β is again equal to 2. However, the two matrix elements go to zero at slightly different energies. In the energy region where the two matrix elements differ significantly, β is expected to differ from 2. In principle, β can have values between 2 and -1. A number of specific cases are worth noting: when $R_{3/2}=0$, $\beta=0$; when $R_{1/2}=0$, $\beta=1$; and when $R_{1/2}=-R_{3/2}$, $\beta=-\frac{2}{3}$.

Manson and Starace[20] have reviewed the subject of energy-dependent photoelectron angular distributions for s subshells. Deviations from $\beta=2$ have been observed in only a few cases. Niehaus and Ruf[21] measured angular distributions for ionization of the $6s$ electron in mercury. They found that β was energy dependent, varying from 2 to 1.25. More recently, several experimental and theoretical groups have studied the $5s \rightarrow \epsilon p$ photoionization of xenon.[22-31] Two of the experiments[28,29] suggest a small "dip" in β at a photon energy of $\sim$32 eV, in the region of the Cooper minimum. Two of the theoretical calculations[24,25] include relativistic effects but only consider single-hole ionization channels and predict a much larger decrease in β from the value 2 than is found experimentally; a third such calculation[27] predicts a smaller decrease in β than is found experimentally. However, Tulkki[31] has recently calculated asymmetry parameters which are in excellent agreement with experiment. These calculations included double-excitation channels on equal footing with the important single-excitation channels using the multichannel multiconfigurational Dirac-Fock (MMCDF) method. Thus in this case, the relativistic (spin-orbit) effects are obscured by the effects of multielectron excitation which are known to be present from studies of satellite spectra in the region of the Xe $5s$ Cooper minimum.[30]

It is indeed surprising to find that, to our knowledge, only one solitary measurement of a photoelectron angular distribution exists for an alkali-metal s state. In 1931 Chaffee[32] reported β of approximately 2 for photoionization of ground-state potassium in the region of $\sim$2400 Å, although he did detect a small residual signal when the light polarization was perpendicular to the electron detection direction. Samson[33] has performed a detailed analysis of these data and concluded that β was equal to 1.55. In 1979 Ong and Manson[10] reanalyzed the Chaffee data to obtain $\beta=1.5\pm0.3$. In order to more rigorously probe spin-orbit effects in the photoionization of the alkali metals, we have measured photoelectron angular distributions for several ns states of cesium.

Figure 1 shows the multiphoton ionization scheme. The photoionization cross sections versus photoelectron energy recently calculated by Lahiri and Manson[34] for the $8s$ and $9s$ states are also shown for illustration. The positions of the Cooper minima are very similar for different principal quantum numbers including the ground state ($n=6$) when plotted versus photoelectron energy.[34] The energy of the photoelectron in the continuum, ϵ, is determined by the photon energy and the ionization of cesium, $\epsilon = 3h\nu - \mathrm{IP}$. Inspection of Fig. 1 shows that the outgoing electron energies are expected to be in the region of the calculated Cooper minima.

Experimentally, an Nd-doped yttrium aluminum garnet–pumped tunable dye laser (Quanta Ray DCR II, PDL2) is used to excite the $8s$, $9s$, $10s$, and $12s$ states of cesium by nonresonant two-photon excitation. It was not possible to study the $11s$ state because of complications of nearby levels (see Ref. 35). A third photon from the same laser beam photoionizes the excited atom. Note that the two-photon excitation results in equal populations of the m_J sublevels, and thus the excited ns states are by definition randomly oriented. The photoelectron angular distributions are therefore not complicated by alignment of the intermediate states. The energy of the photoelectron is determined by its time of flight over a 7-cm path and is detected by a channel-plate charged-particle detector. The angular acceptance of the detection system is $\pm 6.5°$. The plane of polarization of the incident light is rotated with a double Fresnel rhomb which is controlled by a stepping motor. Each angular distribution was collected by averaging 100 laser shots at intervals of 9°. These measurements were difficult due to the small photoionization cross sections for the ns subshells of cesium.[35,36] The small cross section is a result of a Cooper minimum in the continuum, which of course

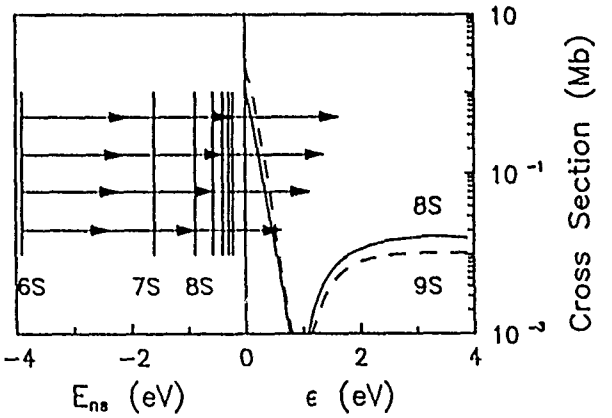

FIG. 1. Illustration of resonantly enhanced three-photon ionization scheme used to study photoelectron angular distributions for ns ($n=8$–12) states of cesium. Also shown are the theoretical photoionization cross sections vs photoelectron energy ϵ of Lahiri and Manson (Ref. 34) for the $8s$ and $9s$ states.

makes the present problem interesting. Several angular-distribution measurements were averaged for each state in order to obtain good signal-to-noise ratios. We should point out that since a signal is only observed when the laser wavelength is in two-photon resonance with an *ns* state, the contribution due to photoionization of dimers should be close to zero. Electron-energy analysis also assures this fact. We note parenthetically that the results of Chaffee[32] were probably affected somewhat by photoionization dimers.

Photoelectron angular distributions for photoionization of *ns* ($n=8$–12) subshells of cesium are shown in Fig. 2. The asymmetry parameters for each angular distribution are obtained using a least-squares method to fit the experimental data by the equation [see Eq. (1)],

$$I(\theta)=1+\beta P_2(\cos\theta). \qquad (4)$$

Note that since $-1\le\beta\le 2$ and $P_2(\cos\theta)=\frac{1}{2}(3\cos^2\theta-1)$, Eq. (4) gives $0\le I(\theta)\le 3$. The β values thus obtained for each state are also indicated in Fig. 2. Identical β values are obtained from $\beta=(R-1)/(1+R/2)$, where R is the ratio of the electron signal recorded at $\theta=0°$ to that at $\theta=90°$. The linear polarization of the laser was $>99.8\%$.

Pindzola[12] has calculated β parameters using the Dirac-Fock approximation in order to obtain the radial-dipole matrix elements used in Eq. (3) for photoionization from the 6*s*, 7*s*, and 8*s* subshells of cesium. When his results for β are plotted versus photoelectron energy, β decreases from 2 to -1 as ϵ goes from 0 to ~ 2 eV. Our measurements for the 8*s* state agree exactly with the theoretical value calculated using the velocity form of the wave function but is $\sim 15\%$ lower than that calculated using the length form.

This study represents the first measurements of photoelectron angular distributions for excited *s* states of an alkali-metal atom. The data clearly show the importance of spin-orbit effects in the photoionization continuum and support the previous theoretical predictions[34] of a Cooper minimum at photoelectron energies just above the threshold for ionization. Further theoretical calculations for the simple case of photoionization of *s* subshells of alkali metals are encouraged. Experimentally, our program is to use two lasers, one to pump the *ns* states and the second to photoionize the *ns* levels at different energies in the continuum. Energy-dependent β parameters for an isolated *ns* state can then be determined as well as the energy dependence of the photoionization cross section. We are also in the process of performing experimental measurements on one-photon ionization of ground state (6*s*) cesium atoms in order to obtain $\sigma(\epsilon)$ and $\beta(\epsilon)$.

This research is sponsored by a grant from the U.S. Office of Naval Research, Grant No. ONR N-00014-87-K-0065, and by the Office of Health and Environmental Research, U.S. Department of Energy under Contract No. DE-AC05-84OR 21400 with Martin Marietta Energy Systems, Inc. L. E. Cuéllar and R. N. Compton have been partially supported by the Science Alliance at the University of Tennessee. We gratefully acknowledge helpful discussions with U. Fano, M. O. Krause, A. F. Starace, F. A. Grimm, and J. W. Cooper.

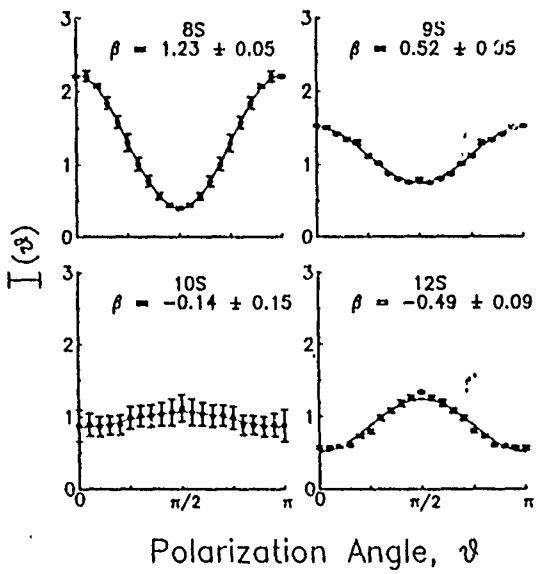

FIG. 2. Photoelectron angular distributions for *ns* ($n=8,9,10,12$) states of cesium. Distributions were measured from 0 to 2π; however, the data from π to 2π are averaged with that from 0 to π and shown here. Solid lines are best fits of data by Eq. (4). Error bars are 1 standard deviation for the average of several angular distributions. The errors in β are $\pm 1\sigma$ from the statistical variance of fit.

[a]Also at Department of Chemistry, The University of Tennessee, Knoxville, TN 37996.

[1]C. N. Yang, Phys. Rev. 74, 764 (1948).

[2]J. Cooper and R. N. Zare, J. Chem. Phys. 48, 942 (1968); *Lectures in Theoretical Physics*, edited by S. Geltman, K. T. Mahanthappa, and W. E. Britten (Gordon and Breach, New York, 1969), Vol. 11C, p. 317.

[3]D. Dill, S. T. Manson, and A. F. Starace, Phys. Rev. Lett. 32, 971 (1974).

[4]A. F. Starace, R.H. Rast, and S. T. Manson, Phys. Rev. Lett. 38, 1522 (1977).

[5]E. S. Chang and K. T. Taylor, J. Phys. B 11, L507 (1978).

[6]S. Shahabi, Phys. Lett. 72A, 212 (1979).

[7]V. Jacobs, J. Phys. B 5, 2257 (1972).

[8]T. E. H. Walker and J. T. Waber, Phys. Rev. Lett. 30, 307 (1973); J. Phys. B 6, 1165 (1973); 7, 674 (1974).

[9]G. V. Marr, J. Phys. B 7, L47 (1974).

[10]W. Ong and S. T. Manson, Phys. Lett. 66A, 17 (1978); Phys. Rev. A 20, 2364 (1979).

[11]K.-N. Huang and A. F. Starace, Phys. Rev. A 19, 2335 (1979).

[12]M. S. Pindzola, Phys. Rev. A 32, 1383 (1985).

[13]E. Fermi, Z. Phys. 59, 680 (1930).

[14]M. J. Seaton, Proc. Roy. Soc. London A 208, 418 (1951).
[15]J. W. Cooper, Phys. Rev. 128, 681 (1962); U. Fano and J. W. Cooper, Rev. Mod. Phys. 40, 441 (1968).
[16]U. Fano, Phys. Rev. 178, 131 (1969); 184, 250 (1969).
[17]G. Baum, M. S. Lubell, and W. Raith, Phys. Rev. Lett. 25, 267 (1970).
[18]U. Heinzmann, J. Kessler, and J. Lorenz, Z. Phys. 240, 42 (1970).
[19]G. Baum, M. S. Lubell, and W. Raith, Phys. Rev. A 5, 1073 (1972).
[20]S. T. Manson and A. F. Starace, Rev. Mod. Phys. 54, 389 (1982).
[21]A. Niehaus and M. W. Ruf, Z. Phys. 252, 84 (1972).
[22]J. L. Dehmer and D. Dill, Phys. Rev. Lett. 37, 1049 (1976).
[23]W. Ong and S. T. Manson, J. Phys. B 11, L65 (1978).
[24]W. R. Johnson and K. T. Cheng, Phys. Rev. Lett. 40, 1167 (1978); Phys. Rev. A 20, 978 (1979).
[25]N. A. Cherepkov, Phys. Lett. 66A, 204 (1978).
[26]M. G. White, S. H. Southworth, P. Kobrin, E. D. Poliakoff, R. A. Rosenberg, and D. A. Shirley, Phys. Rev. Lett. 43, 1661 (1979).
[27]K.-N. Huang and A. F. Starace, Phys. Rev. A 21, 697 (1980).
[28]A. Fahlman, T. A. Carlson, and M. O. Krause, Phys. Rev. Lett. 50, 1114 (1983).
[29]H. Derenbach and V. Schmidt, J. Phys. B 17, L217 (1984).
[30]A. Fahlman, M. O. Krause, and T. A. Carlson, J. Phys. B 17, L217 (1984).
[31]J. Tulkii, Phys. Rev. Lett. 62, 2817 (1989).
[32]M. A. Chaffee, Phys. Rev. 37, 1233 (1931).
[33]J. A. R. Samson (unpublished); (private communication).
[34]J. Lahiri and S. T. Manson, Phys. Rev. A 33, 3151 (1986).
[35]C. E. Klots and R. N. Compton, in *Proceedings of the Third International Conference on Multiphoton Processes, Iraklion, Crete, Greece, 1984*, edited by P. Lambropoulos and S. J. Smith (Springer-Verlag, New York, 1984), pp. 58–66.
[36]C. E. Klots and R. N. Compton, Phys. Rev. A 31, 525 (1985).

PHYSICAL REVIEW A VOLUME 43, NUMBER 11 1 JUNE 1991

Circular dichroism in photoelectron angular distributions for the $7P_{3/2}$ level of cesium

L. E. Cuéllar
Department of Physics and Astronomy, University of Tennessee, Knoxville, Tennessee 37996

C. S. Feigerle
Department of Chemistry, University of Tennessee, Knoxville, Tennessee 37996

H. S. Carman, Jr. and R. N. Compton*
Chemical Physics Section, Oak Ridge National Laboratory, Oak Ridge, Tennessee 37831

(Received 13 November 1990; revised manuscript received 22 February 1991)

Circular dichroism in photoelectron angular distributions (CDAD) is used to examine the alignment of the $7P_{3/2}$ and $7P_{1/2}$ levels of cesium, prepared by absorption of linearly polarized laser radiation. As expected, the $7P_{1/2}$ level exhibits no CDAD, whereas the $7P_{3/2}$ level shows a significant CDAD signal, although smaller than that predicted by theory. The difference between experiment and theory is attributed to m_J mixing due to hyperfine coupling during the finite ionization time of the laser pulse.

INTRODUCTION

In this Rapid Communication, we report an experimental observation of circular dichroism in angular distributions (CDAD) of photoelectrons ejected from an atomic system. Circular dichroism occurs when the responses of a system to left and right circularly polarized light are different. It is often associated with the discrete (bound-bound) absorption of molecules[1,2] that lack a plane or point of symmetry (i.e., they have a chiral center) and is most commonly observed as a difference in the indices of refraction for left and right circularly polarized light. Studies of circular dichrosim are of considerable interest in physics, chemistry, and biology because of the frequent occurrence of chirality in molecules. Bound-continuum absorption has also been predicted to exhibit circular dichrosim,[3-7] providing insight into the dynamics of photoionization processes. Circular dichroic effects have been predicted for angular distributions of photoelectrons ejected from optically active[6,7] and oriented[5] molecules. More recently, Dubs, Dixit, and McKoy[8-10] have proposed that circular dichroism in angular distributions can be used to probe the alignment of atoms and molecules. Alignment (or orientation) of an atom or molecule frequently results from optical excitation using linearly (or circularly) polarized light. A convenient way of studying circular dichroism in angular distributions from aligned systems is to perform a two-color resonance-enhanced multiphoton ionization experiment in which excitation with linearly polarized light is used to produce an aligned intermediate level, which is then ionized using circularly polarized light. The photoelectron signal is measured as a function of the angle between the laser polarization used in the excitation step and the electron collection direction. CDAD is then the difference between photoelectron angular distributions obtained using left and right circularly polarized light for the ionization step. The observed CDAD signal contains information about the alignment of the system under study.[8-10]

Three recent CDAD experiments have been reported for molecular systems. Appling *et al.*[11] used CDAD to probe the alignment of NO molecules excited to the $A\,^2\Sigma^+$ state by linearly polarized light. In a related CDAD study, Winniczek *et al.*[12] probed the alignment of ground-state NO molecules produced by photodissociation of CH_3ONO. CDAD for a *fixed* molecule was reported by Westphal *et al.*,[13] who measured photoelectron angular distributions for CO molecules adsorbed on a Pd(111) crystal (where the CO is oriented with the C atom pointing toward the surface). To our knowledge, no experimental observations of CDAD for an atomic system have been previously reported.

Two groups[14,15] have reported photoelectron angular distributions for resonance-enhanced two-photon ionization (1+1) of cesium via the $7P_{1/2}$ and $7P_{3/2}$ levels, using linearly polarized light for both the excitation and ionization steps. In general, for linearly polarized light, a two-photon ionization process is expected to yield a photoelectron angular distribution of the form[16]

$$I(\theta)=(\sigma/4\pi)[1+\beta_2 P_2(\cos\theta)+\beta_4 P_4(\cos\theta)]\,, \qquad (1)$$

where σ is the total two-photon ionization cross section, P_n are nth-order Legendre polynomials, and β_n are the asymmetry parameters. The β_n coefficients are determined by the radial dipole matrix elements involved in the excitation and ionization transitions and thus contain detailed information about the photoionization process, including the alignment of the intermediate level. If the intermediate level is not aligned (i.e., if all m_J states are equally populated), only terms up to second order in the Legendre polynomial expansion will contribute to the angular distribution. In the case of (1+1) ionization of cesium via the $7P_{1/2}$ level, the $m_J=\pm 1/2$ states are equally populated by absorption of the linearly polarized light and the level is not aligned. For the $7P_{3/2}$ level, however, the $|m_J|=1/2,3/2$ states are unequally populated (only the $m_J=\pm 1/2$ states are excited) by absorption of linearly polarized light, resulting in an aligned level. It is expected therefore that higher-order Legendre polynomials will contribute to the photoelectron angular distribution for

this level. Experimentally, however, it is found[14,15] that the angular distributions observed depend upon the laser-pulse duration. Using a long pulse length ($\approx$400 ns) flashlamp-pumped dye laser, Kaminski, Kessler, and Kollath[14] reported angular distributions for the $7P_{1/2}$ and $7P_{3/2}$ levels which were very similar and adequately described by Eq. (1) including only the second-order term, with $\beta_2 \approx 1.4$. Subsequently, Compton *et al.*[15] measured angular distributions using a nitrogen-pumped dye laser with a shorter pulse duration ($\approx$10 ns). Their results for the $7P_{1/2}$ level agreed well with the results of Kaminski, Kessler, and Kollath,[14] with $\beta_2 \approx 1.3$. However, their results for the $7P_{3/2}$ level differed remarkably from that of Kaminski, Kessler, and Kollath,[14] requiring up to fourth-order terms to fit the data, with $\beta_2 = 1.56$ and $\beta_4 = 0.69$. It was shown theoretically[15] that these differences could be explained by including the effects of hyperfine coupling, which causes a reduction in the alignment of the level during the finite time of the laser pulse.

In a vector model, hyperfine coupling results from the electronic angular momentum vector **J**, precessing about the total angular momentum vector, $\mathbf{F} = \mathbf{J} + \mathbf{I}$, where **I** is the nuclear-spin angular momentum. This precession occurs with a characteristic time of the order $\hbar$ divided by the hyperfine level separation. When the bandwidth of the laser used for excitation is greater than the separations of the relevant hyperfine levels, a nonstationary intermediate state is produced which is a superposition (partially coherent) of hyperfine levels. The time evolution of this nonstationary state results in a mixing of the m_J states, which reduces the initially prepared alignment. Such effects have been described in detail by Fano and Macek[17] and Greene and Zare.[18] The nuclear-spin angular momentum, I, of cesium is $7\hbar/2$ and the hyperfine coupling time is of the order of a few nanoseconds. The alignment measured experimentally will therefore depend upon the duration of the laser pulse. Varying degrees of disalignment thus provides an explanation for the differing results of Kaminski, Kessler, and Kollath[14] and Compton *et al.*[15] for the angular distribution of the $7P_{3/2}$ level of cesium.

In this paper, we present CDAD results for the $7P_{1/2}$ and $7P_{3/2}$ levels of cesium, using a Nd:YAG-pumped dye-laser system (YAG denotes ytrrium aluminum garnet) with $\approx$6-ns pulse duration. Our results are in qualitative agreement with the theoretical predictions of Dubs, Dixit, and McKoy.[9,19] Quantitative differences between experiment and theory are attributed to hyperfine coupling effects during the laser-pulse duration, which were not included in the theory.

EXPERIMENT

The experimental CDAD measurements were performed in an atomic beam apparatus with a base pressure $\approx 10^{-7}$ Torr. A pulsed Nd.YAG-pumped dye laser system (Quanta-Ray DCR,PDL) with a pulse duration of $\approx$6 ns provided the radiation for both the excitation and ionization steps. The output of the dye laser was linearly polarized to $\geq$98% (using a Glan air prism) and was tuned to either the $6S_{1/2} \rightarrow 7P_{1/2}$ or $6S_{1/2} \rightarrow 7P_{3/2}$ transition of atomic cesium. A second laser beam (532 nm, second harmonic of the Nd:YAG) was circularly polarized (using a quarter-wave plate) and counterpropagated with the dye laser beam. In order to obtain a high purity of circular polarization, the polarization of the 532-nm laser beam (which was linearly polarized at the laser exit) was further purified using a Glan air prism, then rotated with a double Fresnel rhomb prior to entering the quarter-wave plate. Right (or left) circular polarization was obtained by rotating the input polarization 45° (or −45°) relative to the quarter-wave plate crystal axis. The two counterpropagating laser beams were crossed by a collimated effusive beam of cesium atoms (oven temperature ~130°C) in the center of a time-of-flight electron-energy analyzer. The time delay between the two laser pulses could be varied with an adjustable optical delay line in the dye laser beam. The time delay was set such that atoms in the ionization volume experienced the full time duration of both laser pulses simultaneously.

Photoelectrons were collected at right angles to both the laser beams and the cesium beam and were energy analyzed by time of flight through a 7-cm drift tube. Stray magnetic fields were reduced to a value below 1 mG by a μ-metal shield lining the vacuum chamber. Electrons were detected with a dual channel-plate multiplier (18-mm diameter) with a concentric-ring anode collector (inner collector, 8-mm diameter; outer collector, 18-mm diameter). Data were obtained with the inner collector which provided a geometric acceptance angle of ±2°. The collector output signal was digitized using a 100-MHz transient digitizer (DSP Technologies 2001A) and transferred via a CAMAC (computer-automated measurement and control) interface to a laboratory computer (Compaq Deskpro 286).

Photoelectron angular distributions were measured by rotating the polarization of the excitation (dye) laser relative to the electron collection direction, while keeping the polarization of the 532-nm ionizing laser fixed. Typically, photoelectron signals were averaged over 100 laser shots and collected at 9° intervals. For the CDAD measurements, the dye laser was attenuated using neutral density filters in order to minimize the one-color (1+1) ionization signal. For all CDAD measurements reported here, the two-color (1+1′) ionization signal was $\geq$100 times that of the one-color (1+1) signal. In addition, the two processes could be distinguished by the difference in electron flight times (a difference of $\approx$30 ns or $\approx$0.39 eV). In order to obtain a CDAD signal, angular distributions were recorded for both left and right circular polarizations of the ionizing laser.

RESULTS AND DISCUSSION

The CDAD signal at a given photoelectron ejection angle (relative to the polarization direction of the excitation laser) is defined[9] as the difference in signals obtained for ionization with left (I_L) and right (I_R) circular polarizations. $I_{\mathrm{CDAD}}(\theta) = I_L(\theta) - I_R(\theta)$. Experimental angular distributions for the $7P_{1/2}$ level of cesium, using left and right circularly polarized light for ionization, are shown in Fig. 1(a). As described above, absorption of linearly polarized light by ground-state cesium atoms produces equal

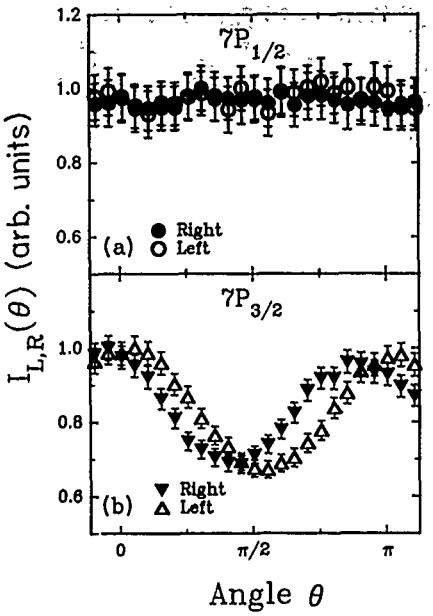

FIG. 1. Photoelectron angular distributions for the (a) $7P_{1/2}$ and (b) $7P_{3/2}$ levels of cesium, using left (L) and right (R) circularly polarized light for ionization. Error bars represent one standard deviation of the signal averaged over several hundred laser shots.

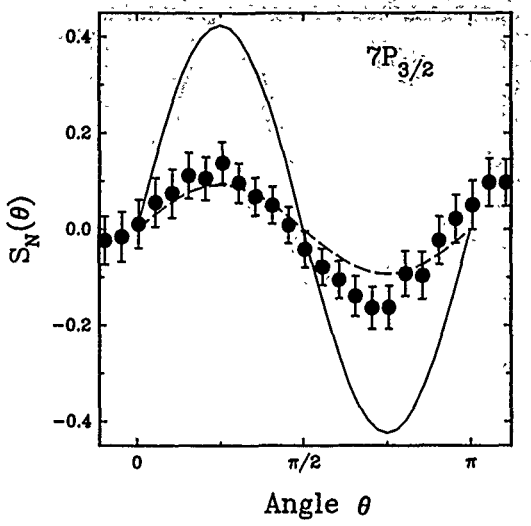

FIG. 2. Experimental and theoretical CDAD signals for the $7P_{3/2}$ level of cesium [normalized according to Eq. (2)]. (●) experimental (error bars represent one standard deviation of the signal averaged over several hundred laser shots); (——) theory (Ref. 19) (without hyperfine corrections); (---) theory including hyperfine corrections (as described in text).

populations of the $m_J = \pm 1/2$ states of the $7P_{1/2}$ level and the atom is therefore (by definition) not aligned. As expected for a system which is not aligned, the angular distributions for ionization with left and right circularly polarized light are found to be identical and $I_{\mathrm{CDAD}}(\theta)$ equals zero at all angles (i.e., there is no circular dichroism). This result, while expected, provided confidence that (i) a high purity of circular polarization of the ionization laser was maintained, (ii) spatial overlap of the two laser beams remained constant during rotation of the excitation-beam polarization, and (iii) the $(1+1)$ contribution to the photoelectron signal was negligible compared to the $(1+1')$ signal.

A similar plot of angular distributions for the $7P_{3/2}$ level is shown in Fig. 1(b). In this case, absorption of linearly polarized light produces an aligned atom (the $|m_J| = 3/2$ and $|m_J| = 1/2$ states are not equally populated) and the angular distributions for ionization by left and right circularly polarized light are clearly different. Figure 2 shows the resulting CDAD signal, which has been normalized to the average of the signals at $\theta = 0$ and $\pi/2$:

$$S_N(\theta) = \frac{I_L(\theta) - I_R(\theta)}{\frac{1}{2}[I(0) + I(\pi/2)]} . \tag{2}$$

Note that, by symmetry, $I_L(\theta) = I_R(\theta) = I(\theta)$ at $\theta = 0$ and $\pi/2$. Also shown in Fig. 2 (solid line) are the theoretical CDAD results of Dubs, Dixit, and McKoy[19] (using the same normalization procedure) for ionization with 532-nm light, based upon the theory of Ref. 9. Qualitatively, the experimental results are consistent with the theoretical predictions. the CDAD signal vanishes at $\theta = 0$ and $\pi/2$ and has a characteristic $\sin(2\theta)$ angular dependence. However, the magnitude of the experimental CDAD signal is considerably smaller than that of the theoretical calculations. Theoretically, the CDAD intensity, $I_{\mathrm{CDAD}}(\theta)$, is given by [10]

$$I_{\mathrm{CDAD}}(\theta) = \sum_L a_L P_L^1(\cos\theta) , \tag{3}$$

where $P_L^1(\cos\theta)$ are associated Legendre polynomials and $a_L = A_L \bar{\bar{\beta}}_L$. Here, A_L are the state multipole moments of the angular momentum distribution (which describe the alignment of the atom) and $\bar{\bar{\beta}}_L$ describe the dynamics of the photoionization event, including the matrix elements and phase shifts of the continuum partial waves.[9,10] For one-photon excitation from an unaligned ground state, only A_2 (the quadrupole moment of the angular momentum distribution) contributes to the alignment of the intermediate level and Eq. (3) reduces to

$$I_{\mathrm{CDAD}}(\theta) = \tfrac{1}{2} A_2 \bar{\bar{\beta}}_2 \sin(2\theta) . \tag{4}$$

The theoretical result of Dubs, Dixit, and McKoy[19] shown in Fig. 2 (solid line) is based upon Eq. (4) with the assumption that no time elapses between excitation and ionization and hence the alignment (A_2) does not change. In the present experiments, as much as ≈ 6 ns can elapse between excitation and ionization. As described above and discussed by Fano and Macek[17] and Greene and Zare,[18] the presence of unresolved hyperfine levels (which are coherently excited) induces a time dependence in the multipole moments of the electronic angular momentum distribution. In general, the hyperfine coupling reduces the alignment initially produced in the excitation step. In the present experiments, the bandwidth of the excitation laser is greater than the splitting of the hyperfine levels of the $7P_{3/2}$ level and a superposition of these hyperfine levels ($F = 5, 4, 3, 2$) is excited. A decrease in alignment caused by hyperfine coupling may therefore affect the CDAD results.

In order to quantitatively estimate the effect of hyperfine coupling on the CDAD results, the time dependence of A_2 was calculated using the theory of Fano and Macek.[17,18] In the actual CDAD experiment, each Cs atom will undergo a different amount of depolarization depending on the time between excitation and ionization, and the measured alignment will be a convolution of the time dependence of the depolarization, the ionization rate, and the laser power and pulse shape. In order to simplify the calculation considerably, we calculated the average value of A_2 in the "long-time limit,"[18] which is applicable when ionization occurs over a time period which is much longer than the time of precession of **J** about **F**. In this limit, the average value of A_2 is given by[18]

$$\langle A_2(t)\rangle = A_2(0)\sum_{F=2}^{5}\frac{(2F+1)^2}{(2I+1)}\begin{Bmatrix} F & F & 2 \\ J & J & I \end{Bmatrix}^2 . \qquad (5)$$

Evaluation of the $6j$-symbols and summation over F yields $\langle A_2(t)\rangle = 0.219 A_2(0)$. Therefore the theoretical CDAD results of Dubs, Dixit, and McKoy,[19] which were calculated assuming $A_2 = A_2(0)$, were multiplied by 0.219 to give the dashed curve shown in Fig. 2. As can be seen, the inclusion of hyperfine depolarization (even in the approximation of the long-time limit) results in much better, although not statistically perfect, agreement between theory and experiment. The remaining discrepancy is not suprising in view of the fact that the long-time limit used to obtain Eq. (5) only roughly approximates the 6-ns laser pulse duration used for the experiments.

We conclude that CDAD is indeed a sensitive method for measuring the alignment of atomic systems and should be a useful technique in many areas of atomic and molecular physics. Further experiments are planned to measure CDAD in the absence of hyperfine depolarization using high-resolution diode lasers to excite single hyperfine levels of heavy atoms.

ACKNOWLEDGMENTS

This research is sponsored by a grant from the U.S. Office of Naval Research, Grant No. ONR N-00014-87-K-0065 and by the Office of Health and Environmental Research, U.S. Department of Energy, under Contract No. DE-AC05-840R21400 with Martin Marietta Energy Systems, Inc. We would like to thank R. L. Dubs, S. N. Dixit, and V. McKoy for helpful discussions and for providing the results of their calculations prior to publication.

*Also at Department of Chemistry, University of Tennessee, Knoxville, TN 37996.

[1]E. U. Condon, W. Altar, and H. Eyring, J. Chem. Phys. **5**, 753 (1937).

[2]E. U. Condon, Rev. Mod. Phys. **9**, 432 (1937).

[3]N. A. Cherepkov, Chem. Phys. Lett. **87**, 344 (1982).

[4]R. Parzyński, Acta Phys. Polonica **A57**, 49 (1980).

[5]B. Ritchie, Phys. Rev. A **12**, 567 (1975).

[6]B. Ritchie, Phys. Rev. A **13**, 1411 (1976).

[7]B. Ritchie, Phys. Rev. A **14**, 359 (1976).

[8]R. L. Dubs, S. N. Dixit, and V. McKoy, Phys. Rev. Lett. **54**, 1249 (1985).

[9]R. L. Dubs, S. N. Dixit, and V. McKoy, J. Chem. Phys. **85**, 656 (1986).

[10]R. L. Dubs, S. N. Dixit, and V. McKoy, J. Chem. Phys. **85**, 6267 (1986).

[11]J. R. Appling, M. G. White, T. M. Orlando, and S. L. Anderson, J. Chem. Phys. **85**, 6803 (1986); J. R. Appling, M. G. White, R. L. Dubs, S. N. Dixit, and V. McKoy, J. Chem. Phys. **87**, 6927 (1987).

[12]J. W. Winniczek, R. L. Dubs, J. R. Appling, V. McKoy, and M. G. White, J. Chem. Phys. **90**, 949 (1989).

[13]C. Westphal, J. Bansmann, M. Getzlaff, and G. Schönhense, Phys. Rev. Lett. **63**, 151 (1989).

[14]H. Kaminski, J. Kessler, and K. J. Kollath, Phys. Rev. Lett. **45**, 1161 (1980).

[15]R. N. Compton, J. A. D. Stockdale, C. D. Cooper, X. Tang, and P. Lambropoulos, Phys. Rev. A **30**, 1766 (1984).

[16]P. Lambropoulos, Adv. At. Mol. Opt. Phys. **12**, 87 (1976).

[17]U. Fano and J. H. Macek, Rev. Mod. Phys. **45**, 553 (1973).

[18]C. H. Greene and R. N. Zare, Annu. Rev. Phys. Chem. **33**, 119 (1982).

[19]R. L. Dubs, S. N. Dixit, and V. McKoy (unpublished).